

# Sequential activation of transcriptional repressors promotes progenitor commitment by silencing stem cell identity genes

Noemi Rives-Quinto<sup>1</sup>, Hideyuki Komori<sup>1</sup>, Cyrina M Ostgaard<sup>1,2</sup>, Derek H Janssens<sup>1†</sup>, Shu Kondo<sup>3</sup>, Qi Dai<sup>4</sup>, Adrian W Moore<sup>5</sup>, Cheng-Yu Lee<sup>1,2,6\*</sup>

<sup>1</sup>Life Sciences Institute, University of Michigan, Ann Arbor, United States;

<sup>2</sup>Department of Cell and Developmental Biology, University of Michigan Medical School, Ann Arbor, United States; <sup>3</sup>Invertebrate Genetics Laboratory, National Institute of Genetics, Mishima, Japan; <sup>4</sup>Department of Molecular Biosciences, The Wenner-Gren Institute, Stockholm University, Stockholm, Sweden; <sup>5</sup>Riken Center for Brain Science, Wako, Japan; <sup>6</sup>Division of Genetic Medicine, Department of Internal Medicine and Comprehensive Cancer Center, University of Michigan Medical School, Ann Arbor, United States

**Abstract** Stem cells that indirectly generate differentiated cells through intermediate progenitors drives vertebrate brain evolution. Due to a lack of lineage information, how stem cell functionality, including the competency to generate intermediate progenitors, becomes extinguished during progenitor commitment remains unclear. Type II neuroblasts in fly larval brains divide asymmetrically to generate a neuroblast and a progeny that commits to an intermediate progenitor (INP) identity. We identified Tailless (Tll) as a master regulator of type II neuroblast functional identity, including the competency to generate INPs. Successive expression of transcriptional repressors functions through Hdac3 to silence *tll* during INP commitment. Reducing repressor activity allows re-activation of Notch in INPs to ectopically induce *tll* expression driving supernumerary neuroblast formation. Knocking-down *hdac3* function prevents downregulation of *tll* during INP commitment. We propose that continual inactivation of stem cell identity genes allows intermediate progenitors to stably commit to generating diverse differentiated cells during indirect neurogenesis.

\*For correspondence:  
leecheng@umich.edu

Present address: <sup>†</sup>Basic Sciences Division, Fred Hutchinson Cancer Research Center, Seattle, United States

Competing interests: The authors declare that no competing interests exist.

Funding: See page 18

Received: 20 February 2020

Accepted: 25 November 2020

Published: 26 November 2020

Reviewing editor: Claude Desplan, New York University, United States

© Copyright Rives-Quinto et al. This article is distributed under the terms of the [Creative Commons Attribution License](https://creativecommons.org/licenses/by/4.0/), which permits unrestricted use and redistribution provided that the original author and source are credited.

## Introduction

Indirect generation of differentiated cell types through intermediate progenitors allows tissue-specific stem cells to scale their progeny output to accommodate the development of appropriately sized organs in proportion to organism sizes. Indirect neurogenesis by the outer subventricular zone (OSVZ) neural stem cells drives the evolution of lissencephalic brains to gyrencephalic brains in vertebrates (Cárdenas and Borrell, 2020). The competency to generate intermediate progenitors and the maintenance of an undifferentiated state must be coordinately downregulated in stem cell progeny to ensure generation of differentiated cell types. Polycomb-mediated gene repression is thought to inactivate stem-cell-specific genes during differentiation (Tsuboi et al., 2019). However, loss of function of Polycomb Repressive Complex 2 (PRC2) did not lead to intermediate progenitors reverting into neural stem cells (Abduslamoglu et al., 2019). Thus, the mechanisms that extinguish stem cell functionality during progenitor commitment remains poorly understood.

Two distinct neuroblast lineages function together to generate the number of neurons requisite for the development of adult fly brains (*Farnsworth and Doe, 2017; Homem et al., 2015; Janssens and Lee, 2014*). Similar to ventricular zone neural stem cells, type I neuroblasts undergo direct neurogenesis. Type I neuroblasts repeatedly undergo asymmetric division to generate one daughter cell that remains a neuroblast and one sibling cell (ganglion mother cell [GMC]) that divides once to generate two neurons. By contrast, type II neuroblasts undergo indirect neurogenesis, similar to OSVZ neural stem cells. Type II neuroblasts continually undergo asymmetric division to self-renew and to generate a sibling cell that commits to an intermediate progenitor (INP) identity (*Bello et al., 2008; Boone and Doe, 2008; Bowman et al., 2008*). The Sp family transcription factor Buttonhead (Btd) and the ETS-1 transcription factor PointedP1 (PntP1) are specifically expressed in type II neuroblasts (*Komori et al., 2014b; Xie et al., 2014; Zhu et al., 2011*). Btd and PntP1 expression levels decrease as a newly generated immature INP transitions into a non-*Ase*<sup>-</sup> immature INP. Three to four hrs after this transition, an *Ase*<sup>-</sup> immature INP upregulates *Ase* expression as it progresses through INP commitment. Once INP commitment is complete, an *Ase*<sup>+</sup> immature INP transitions into an INP that undergoes six to eight rounds of asymmetric division. These molecularly defined intermediate stages during INP commitment provide critical landmarks to investigate the mechanisms that extinguish the activity of type II neuroblast functional identity genes.

Notch signaling maintains type II neuroblasts in an undifferentiated state, partially by poisoning transcription of the master regulator of differentiation *earmuff* (*erm*) (*Janssens et al., 2017*). During asymmetric neuroblast division, the TRIM-NHL protein Brain tumor (Brat) segregates into the newly generated immature INP and targets transcripts encoded by Notch downstream effector genes for RNA decay (*Bello et al., 2006; Betschinger et al., 2006; Komori et al., 2018; Lee et al., 2006b; Xiao et al., 2012*). *brat*-null brains accumulate thousands of supernumerary type II neuroblasts that originate from the reversion of newly generated immature INPs due to defects in the downregulation of Notch signaling (*Komori et al., 2014a*). In parallel to Brat, the nuclear protein Insensible (*Insb*) inhibits the activity of Notch downstream effector proteins during asymmetric neuroblast division, and *Insb* overexpression efficiently triggers premature differentiation in type II neuroblasts (*Komori et al., 2018*). This multi-layered gene control allows for the onset of *Erm* expression, coinciding with the termination of PntP1 expression. *Erm* expression is maintained in immature INPs but becomes downregulated in INPs (*Janssens et al., 2014*). *Erm* belongs to a family of transcription factors that are highly expressed in neural progenitors and can bind histone deacetylase 3 (Hdac3) (*Hirata et al., 2006; Koe et al., 2014; Levkowitz et al., 2003; Weng et al., 2010*). *Erm* prevents INP reversion by repressing gene transcription. In *erm*-null brains, INPs spontaneously revert to type II neuroblasts; however, this phenotype can be suppressed by knocking-down Notch function (*Weng et al., 2010*). Thus, *Erm* likely inactivates type II neuroblast functionality genes by promoting histone deacetylation.

By comparing mRNAs enriched in type II neuroblasts or immature INPs, we identified *tailless* (*tll*) as a master regulator of type II neuroblast functional identity. *Tll* is expressed in type II neuroblasts but not in INPs; moreover, *Tll* is necessary and sufficient for type II neuroblast functionality. *Tll* overexpression is sufficient to transform type I neuroblasts into type II neuroblasts, as indicated by changes in gene expression and an acquired competence for generating INPs. We identified *hamlet* (*ham*) as a new negative regulator of type II neuroblast maintenance. *ham* is expressed after *erm* in immature INP during INP commitment, and *Erm* and *Ham* function through Hdac3 to continually inactivate *tll*. Sequential inactivation during INP commitment suppresses *tll* activation by Notch signaling in INPs. We propose that silencing of the master regulator of stem cell functional identity allows intermediate progenitors to stably commit to the generation of differentiated cell types without reacquiring stem cell functionality.

## Results

### A novel transient over-expression strategy to identify regulators of type II neuroblast functional identity

Genes that regulate neuroblast functional identity should be expressed in type II neuroblasts and become rapidly downregulated in *Ase*<sup>-</sup> and *Ase*<sup>+</sup> immature INPs in wild-type brains (*Figure 1A*). To

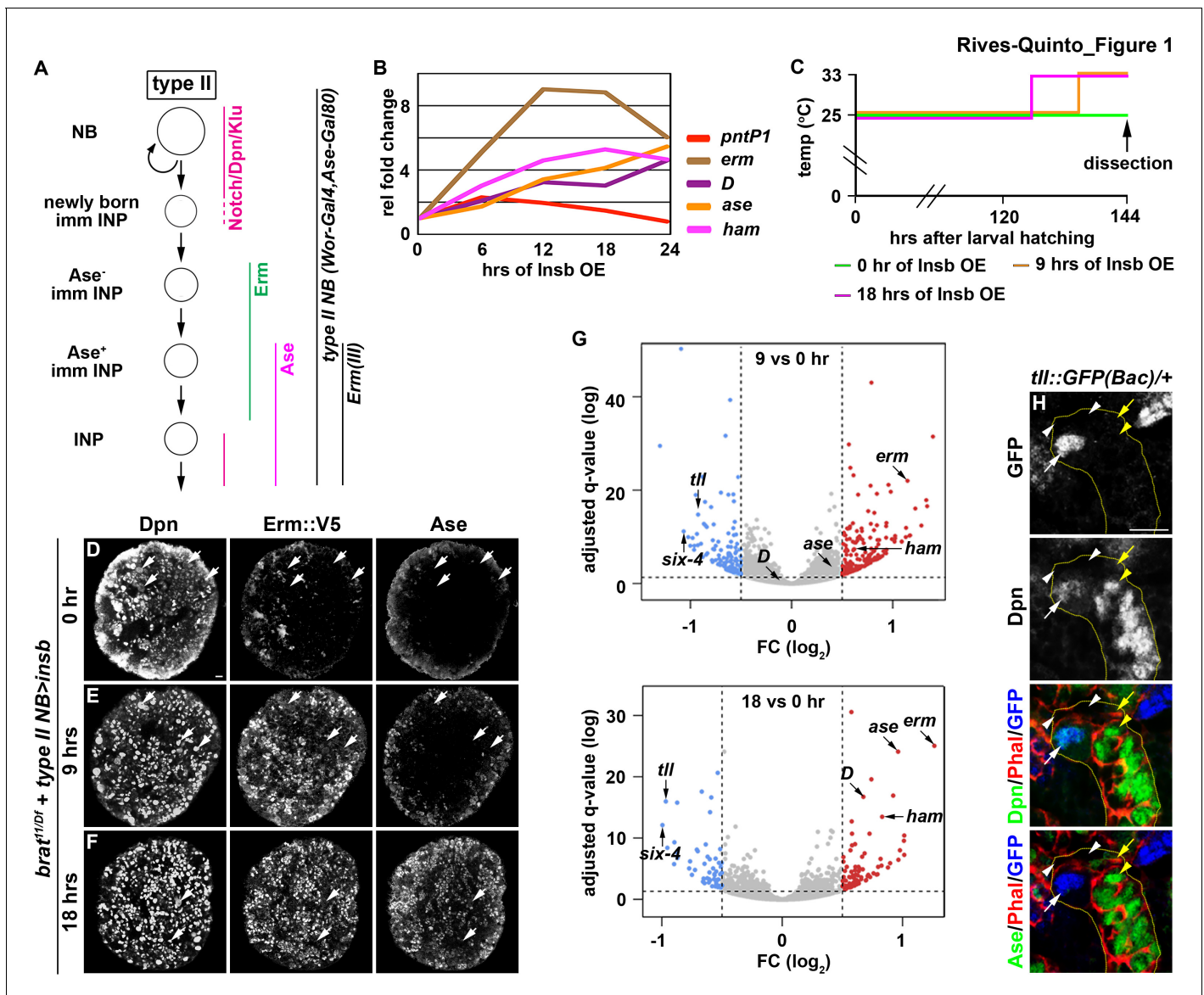


**Figure 1.** Identification of candidate regulators of type II neuroblast functional identity. (A) A diagram of the type II neuroblast lineage showing the expression patterns of genes and *Gal4* drivers used throughout this study. (B) Gene transcription profiles of *brat*-null brains transiently overexpressing *Insb* driven by a type II neuroblast *Gal4*. Supernumerary type II neuroblasts in *brat*-null brains transiently overexpressing *Insb* displayed patterns of gene transcription that are indicative of immature INPs undergoing INP commitment in wild-type brains. (C) A strategy to induce synchronized INP commitment in supernumerary type II neuroblasts in *brat*-null brains. Larvae carrying a *UAS-insb* transgene and a type II neuroblast *Gal4* were collected and aged at 25°C. One third of larvae were shifted to 33°C at 126 or 135 hr after hatching to induce high levels of transient *Insb* expression, and the last one-third remained at 25°C serving as the source enriched for type II neuroblast-specific transcripts (time 0). (D–F) Images of *brat*-null brains transiently overexpressing *Insb* driven by a type II neuroblast *Gal4* for 0, 9, or 18 hr. Transient overexpression of *Insb* first induced *Erm* and then *Ase* expression in supernumerary type II neuroblasts in *brat*-null brains. (G) Volcano plots showing fold-change of gene expression in *brat*-null brains transiently overexpressing *Insb* for 9 or 18 hr. (H) Tll expression pattern in the type II neuroblast lineage. The *tll::GFP(Bac)/+* transgene revealed the expression of endogenous Tll in type II neuroblasts but not in immature INPs and INPs. The following labeling applies to all images in this figure: yellow dashed line encircles a type II neuroblast lineage; white arrow: type II neuroblast; white arrowhead: *Ase*<sup>-</sup> immature INP; yellow arrow: *Ase*<sup>+</sup> immature INP; yellow arrowhead: INP. Scale bar, 10 μm.

The online version of this article includes the following source data and figure supplement(s) for figure 1:

**Figure supplement 1.** Time-course analysis of transient *Insb* overexpression in *brat*-null brains.

**Figure supplement 1—source data 1.** Quantification of total type II neuroblasts or INPs per *brat*-null brain lobe that transiently overexpressed *Insb*.

enrich for transcripts that fulfill these criteria, we tested if transient *Insb* overexpression induces supernumerary type II neuroblasts in *brat*-null brains to synchronously transition into INPs as in wild-type brains. The combination of *Wor-Gal4*, *AseGal80*, which is only active in type II neuroblasts, and *Tub-Gal80<sup>ts</sup>*, which loses its inhibitory effect on Gal4 activity under non-permissive temperatures, allows for spatial and temporal control of *Insb* overexpression in all type II neuroblasts. We allowed larvae to grow at 25°C, and induced transient *Insb* overexpression for 6, 12, 18, or 24 hr by shifting the larvae to a non-permissive temperature of 33°C. Larvae that remained at 25°C for the duration of this experiment served as the control (time 0). We assessed the effect of this transient over-expression strategy on cell identity by quantifying the total type II neuroblasts and INPs per brain lobe based on Deadpan (*Dpn*) and *Ase* expression (**Figure 1A**). Overexpressing *Insb* for 6 hr did not significantly affect the supernumerary neuroblast phenotype in *brat*-null brains (**Figure 1—figure supplement 1A**). By contrast, 12 or more hours of *Insb* overexpression led to a time-dependent decrease in supernumerary type II neuroblasts and a corresponding increase in INPs. These results demonstrate that transient *Insb* overexpression can induce supernumerary type II neuroblasts to synchronously transition into INPs in *brat*-null brains.

We next assessed if supernumerary type II neuroblasts transiently overexpressing *Insb* transition through identical intermediate stages to become INPs in *brat*-null brains as they do in wild-type brains (**Figure 1A**). We found that *pntP1* mRNA levels increased within the first 6 hr of *Insb* overexpression, and then continually declined (**Figure 1B**). By contrast, *erm* transcription rapidly increased in the first 12 hr of *Insb* overexpression, plateauing between 12 and 18 hr. *ase* transcription showed little change in the first 6 hr of *Insb* overexpression, and then steadily increased between 12 and 24 hr. The combined temporal patterns of *pntP1*, *erm*, and *ase* transcription strongly suggest that type II neuroblasts transiently overexpressing *Insb* for 6 hr in *brat*-null brains are at an equivalent stage as a newly generated immature INP transitioning to an *Ase*<sup>-</sup> immature INP in wild-type brains. *brat*-null type II neuroblasts are at a stage equivalent to (1) *Ase*<sup>-</sup> immature INPs following 6–12 hr of *Insb* overexpression and (2) *Ase*<sup>+</sup> immature INPs following 12–24 hr of *Insb* overexpression. We examined the expression of endogenous *Erm* in *brat*-null type II neuroblasts transiently overexpressing *Insb* to confirm their identity. We generated an *erm::V5* allele by inserting a V5 epitope at the C-terminus of the *erm* reading frame, and showed that *Erm::V5* recapitulates the published endogenous *Erm* expression pattern that we previously described (**Figure 1—figure supplement 1B**; *Janssens et al., 2014*). Indeed, following 9 hr of *Insb* overexpression most type II neuroblasts in *brat*-null brains expressed cell identity markers indicative of *Ase*<sup>-</sup> immature INPs (*Erm::V5*<sup>+</sup>*Ase*<sup>-</sup>), whereas after 18 hr of *Insb* overexpression they expressed markers indicative of *Ase*<sup>+</sup> immature INPs (*Erm::V5*<sup>+</sup>*Ase*<sup>+</sup>) (**Figure 1C–F**). These data indicate that supernumerary type II neuroblasts transiently overexpressing *Insb* indeed transition through identical intermediate stages during INP commitment in *brat*-null brains as in wild-type brains.

We predicted that a candidate regulator of type II neuroblast functional identity should become downregulated in *brat*-null brains following 9 and 18 hr of *Insb* overexpression. By sequencing mRNA in triplicate following the transient over-expression strategy (**Figure 1C**), we identified 76 genes that were reproducibly downregulated by 1.5-fold or more in *brat*-null brains overexpressing *Insb* for 9 hr (**Figure 1G**). Of these genes, *tll* was the most downregulated; similarly, *tll* was the most downregulated gene in *brat*-null brains overexpressing *Insb* for 18 hr. We validated the *tll* expression pattern in the type II neuroblast lineage using a bacterial artificial chromosome (BAC) transgene [*tll::GFP(Bac)*] where green fluorescent protein (GFP) is fused in frame with the *tll* reading frame. Consistent with previous study (*Bayraktar and Doe, 2013*), we detected *Tll::GFP* in type II neuroblasts but not in immature or mature INPs (**Figure 1H**). *Tll::GFP* expression is also detected in type I neuroblasts in the brain and in the ventral nerve cord, but at a significantly lower level than in type II neuroblasts (**Figure 1—figure supplement 1C–E**). Thus, *tll* is an excellent candidate for regulating type II neuroblast functionality.

### ***tll* is a master regulator of type II neuroblast functional identity**

We defined the type II neuroblast functional identity as the maintenance of an undifferentiated state and the competency to generate INPs. We first tested whether *tll* is required for maintaining type II neuroblasts in an undifferentiated state by overexpressing a *UAS-tll<sup>RNAi</sup>* transgene in the type II neuroblast lineage under the control of the *Wor-Gal4*, *Ase-Gal80* driver (**Figure 2A**). Whereas control brains always contained eight type II neuroblasts per lobe, brains with *tll* function knocked down

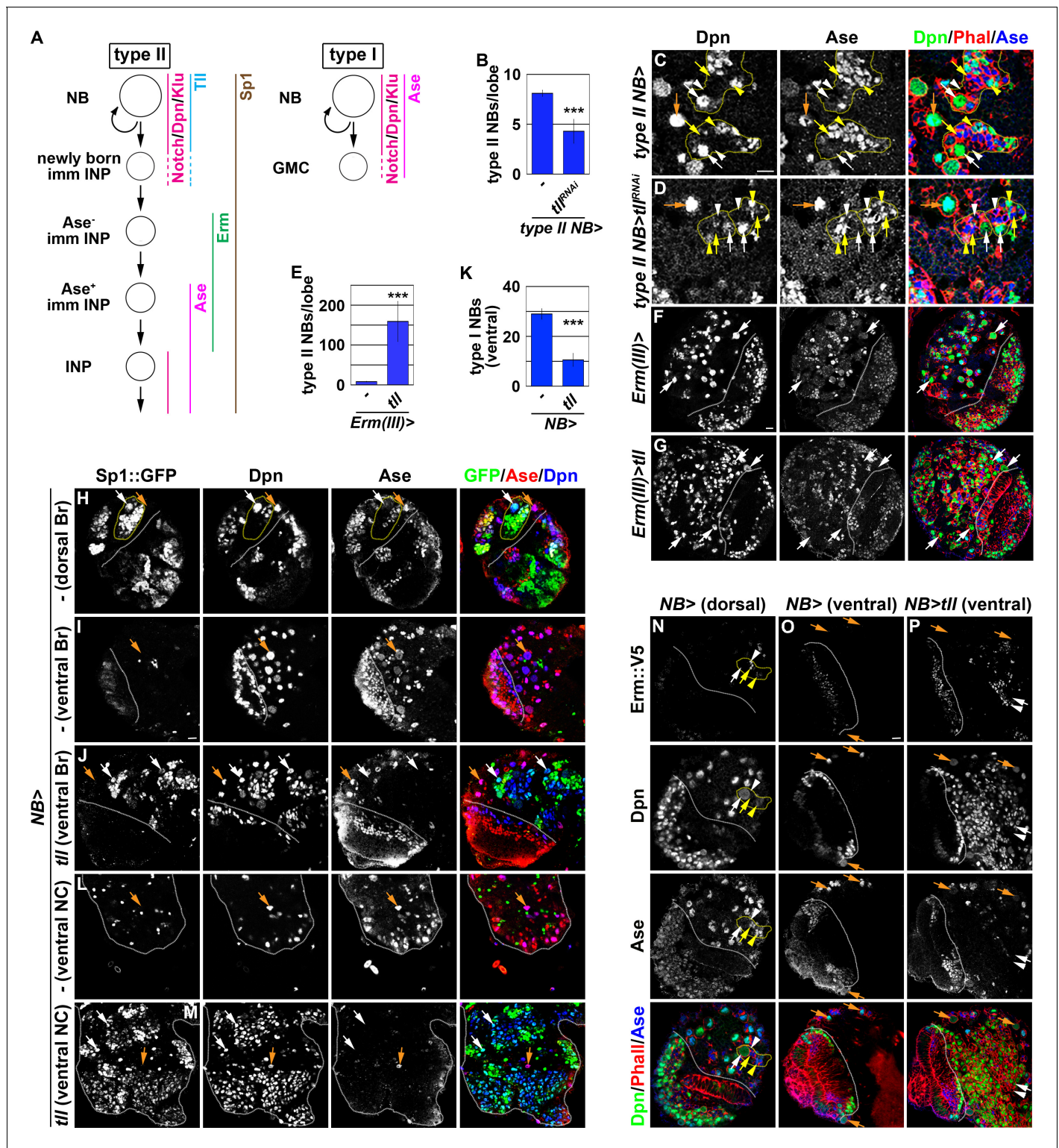


**Figure 2.** *tll* is necessary and sufficient for type II neuroblast functional identity. (A) A diagram showing the expression patterns of genes in the type I and II neuroblast lineages. (B) Quantification of total type II neuroblasts per brain lobe that overexpressed a UAS-*tll*<sup>RNAi</sup> transgene driven by a type II neuroblast Gal4. Knocking-down *tll* function reduced the number of type II neuroblasts from 8 to 4 per brain lobe. (C–D) Images of brains that overexpressed a UAS-*tll*<sup>RNAi</sup> transgene driven by a type II neuroblast Gal4. Knocking-down *tll* function led to premature differentiation in type II neuroblast as indicated by reduced cell diameter and ectopic Ase expression but did not affect the maintenance of type I neuroblasts. (E) Quantification of total type II neuroblasts per brain that overexpressed a UAS-*tll* transgene driven by an INP Gal4. *tll* overexpression in INPs led to

Figure 2 continued on next page

## Figure 2 continued

supernumerary type II neuroblast formation. (F–G) Images of brains that overexpressed a *UAS-tll* transgene driven by an INP Gal4. (H–I) Images of *Sp1::GFP(Bac)* brains. *Sp1::GFP* is detected in most cells in all type II neuroblast lineages that are exclusively located in the dorsal brain region, and is detected in few neurons in type I neuroblast lineages in the ventral brain region. (J) Images of the ventral region of *Sp1::GFP(Bac)* brains that overexpressed a *UAS-tll* transgene driven by a pan-neuroblast Gal4 (*Wor-Gal4*). *Tll* overexpression transforms type I neuroblasts (*Ase*<sup>+</sup>*Sp1::GFP*) in the ventral brain region into type II neuroblasts (*Ase*<sup>-</sup>*Sp1::GFP*). (K) Quantification of total ventral type I neuroblasts per brain lobe that overexpressed a *UAS-tll* transgene driven by a pan-neuroblast Gal4. *Tll* overexpression transforms 66% of type I neuroblasts in the ventral brain region into type II neuroblasts. (L–M) Images of the thoracic segments on the ventral nerve cord of *Sp1::GFP(Bac)* larvae that overexpressed a *UAS-tll* transgene driven by a pan-neuroblast Gal4 (*Wor-Gal4*). *Tll* overexpression transforms type I neuroblasts in the thoracic segments into type II neuroblasts. (N–O) Images of dorsal and ventral regions of *erm::V5* brains. *Erm::V5* is detected in immature INPs in type II neuroblast lineages but is undetectable in type I neuroblast lineages in the ventral region of larval brain. (P) Images of *erm::V5* brains that overexpressed a *UAS-tll* transgene driven by a pan-neuroblast Gal4. *Tll* overexpression induced type I neuroblasts in the ventral-medial region of the brain to generate supernumerary type II neuroblasts interspersed with *Erm::V5*<sup>+</sup> immature INPs. The following labeling applies to all images in this figure: white dashed line separates the optic lobe from the brain; yellow dashed line encircles a type II neuroblast lineage; white arrow: type II neuroblast; white arrowhead: *Ase*<sup>-</sup> immature INP; yellow arrow: *Ase*<sup>+</sup> immature INP; yellow arrowhead: INP; orange arrow: type I neuroblast. Br: brain. NC: nerve cord. Scale bar, 10 μm. Bar graphs are represented as mean ± standard deviation. p-values: \*\*\*<0.005.

The online version of this article includes the following source data for figure 2:

**Source data 1.** Quantification of total type II neuroblasts per brain lobe that overexpressed a *UAS-tll*<sup>RNAi</sup> transgene.

**Source data 2.** Quantification of total type II neuroblasts per brain that overexpressed a *UAS-tll* transgene.

**Source data 3.** Quantification of total ventral type I neuroblasts per brain lobe that overexpressed a *UAS-tll* transgene.

contained  $4.3 \pm 1.2$  type II neuroblasts per lobe ( $n = 10$  brains per genotype) (**Figure 2B**). A closer examination revealed that the remaining *tll* mutant neuroblasts showed reduced cell diameters and ectopically expressed *Ase*, two characteristics typically associated with INPs in the type II neuroblast lineage (**Figure 2A, C and D**). This result indicated that *tll* is required for maintaining type II neuroblasts in an undifferentiated state. We next tested whether *tll* is sufficient to re-establish a type II neuroblast-like undifferentiated state in INPs by misexpressing a *UAS-tll* transgene under the control of *Erm-Gal4(III)* (**Figure 1A**). Brains with *tll* misexpressed in INPs contained  $150 \pm 50$  type II neuroblasts per lobe, whereas control brains always contained eight type II neuroblasts per lobe ( $n = 10$  brains per genotype) (**Figure 2E–G**). Thus, *Tll* misexpression is sufficient to revert INPs to type II neuroblasts. These data together led us to conclude that *tll* is necessary and sufficient for maintaining type II neuroblasts in an undifferentiated state.

As *tll* is required to maintain type II neuroblasts in an undifferentiated state, direct assessment of its role in regulating the competency to generate INPs is not possible. As an alternative, we tested whether *Tll* overexpression is sufficient to induce ectopic type II neuroblast formation in the ventral brain region and in the ventral nerve cord that exclusively consist of type I neuroblasts. To unambiguously distinguish the two types of neuroblasts, we searched for robust protein markers of type II neuroblasts and their progeny. As *Sp1* mRNA is uniquely detected in type II neuroblasts (**Yang et al., 2016**), we evaluated *Sp1* protein expression using an *Sp1::GFP(Bac)* transgene. We found that *Sp1::GFP* marks type II neuroblasts and most of their progeny that are found exclusively in the dorsal brain region (**Figure 2H**). *Sp1::GFP* is detected in some neurons but never in type I neuroblasts in the ventral brain region and in the ventral nerve cord (**Figure 2I and L**). Thus, *Sp1::GFP* is a new marker for the type II neuroblast lineage (**Figure 2A**). We overexpressed a *UAS-tll* transgene under the control of a pan-neuroblast driver (*Wor-Gal4*) in larval brains carrying the *Sp1::GFP(Bac)* transgene. While the ventral region of control brains contains  $29 \pm 2.1$  type I neuroblasts, the same region of the brains overexpressing *Tll* contains  $10.6 \pm 2.5$  type I neuroblasts and hundreds of ectopic type II neuroblasts ( $n = 10$  brains per genotype) (**Figure 2I–K**). This result strongly suggests that *Tll* overexpression transforms greater than 60% of type I neuroblasts in the ventral brain region into type II neuroblasts. Similarly, *Tll* overexpression also induced hundreds of supernumerary type II neuroblasts in the ventral nerve cord ( $n = 10$  brains per genotype) (**Figure 2L and M**). Thus, ectopic *tll* expression is sufficient to molecularly transform type I neuroblasts into type II neuroblasts.

Next, we tested if type I neuroblasts overexpressing *tll* can generate immature INPs that are marked by *Erm::V5* expression (**Figure 2A and N**). We reproducibly observed *Erm::V5*<sup>+</sup> immature INPs in the ventral-medial region of the brain overexpressing *Tll*, but not in the ventral-lateral brain region (**Figure 2O and P**). This result strongly suggests that progeny of transformed type II

neuroblasts in the ventral-medial brain region assume an immature INP identity and then revert into supernumerary type II neuroblasts. By contrast, progeny of transformed type II neuroblasts in the ventral-lateral brain region appeared to rapidly revert into supernumerary neuroblasts instead of assuming an immature INP identity. Thus, *tll* overexpression is sufficient to molecularly and functionally transform type I neuroblasts into type II neuroblasts, and that *tll* is a master regulator of type II neuroblast functional identity.

## Ham is a new regulator of INP commitment

A previous study found that Suppressor of Hairless, the DNA-binding partner of Notch, binds the *tll* locus in larval brain neuroblasts, suggesting that *tll* is a putative Notch target (Zacharioudaki et al., 2016). Thus, mechanisms likely exist to silence *tll* during INP commitment, preventing re-activation of Notch signaling in INPs from ectopically inducing TII expression and driving supernumerary type II neuroblast formation (Figure 2A). We predicted that genes required for silencing *tll* during INP commitment should become upregulated in *brat*-null brains following 9 and 18 hr of *Insb* overexpression, and mutations in these genes should lead to supernumerary type II neuroblast formation due to ectopic *tll* expression in INPs. From our RNA sequencing dataset, we identified genes that encode transcription factors and are upregulated in *brat*-null brains overexpressing *Insb* for 9 or 18 hr. These transcription factors include *Erm*, *Dichaete* (*D*), *Ase*, and *Hamlet* (*Ham*) (Figure 1G). Reverse transcriptase PCR confirmed that the transcript levels of these genes indeed become upregulated in *brat*-null brains overexpressing *Insb* (Figure 1B). Thus, these genes are candidates for inactivating *tll* during INP commitment.

We tested if any of the candidate genes is required for inactivating *tll* expression during INP commitment by knocking-down their function in *erm* hypomorphic (*erm<sup>hyp</sup>*) brains. *erm<sup>hyp</sup>* brains display a low frequency of INP reversion to type II neuroblasts, and provides a sensitized genetic background for identifying genes required to prevent INP reversion to type II neuroblasts (Janssens et al., 2017). Because ectopic *tll* expression in INPs leads to supernumerary type II neuroblast formation, reducing the function of genes that inactivate *tll* should enhance the supernumerary neuroblast phenotype in *erm<sup>hyp</sup>* brains. We found that *erm<sup>hyp</sup>* brains alone contained  $31.5 \pm 6.8$  type II neuroblasts per lobe ( $n = 10$  brains) (Figure 3A). Although reducing the function of most candidate genes did not enhance the supernumerary neuroblast phenotype in *erm<sup>hyp</sup>* brains, knocking-down *ham* function with two different *UAS-RNAi* transgenes reproducibly enhanced the phenotype ( $n = 10$  brains per transgene) (Figure 3A). Consistent with the effect of reducing *ham* function by RNAi, the heterozygosity of a deficiency that deletes the entire *ham* locus also enhanced the supernumerary neuroblast phenotype in *erm<sup>hyp</sup>* brains (data not presented). Thus, *ham* likely plays a role in preventing INPs from reverting to supernumerary type II neuroblasts.

*ham* is the fly homolog of the vertebrate *Prdm16* gene that encodes a transcription factor and has been shown to play a key role in regulating cell fate decisions in multiple stem cell lineages (Baizabal et al., 2018; Harms et al., 2015; Moore et al., 2002; Shimada et al., 2017). A previous study concluded that *ham* regulates INP proliferation but does not play a role in suppressing supernumerary type II neuroblast formation (Eroglu et al., 2014). The discrepancy between our findings and the published observations might be due to the *ham<sup>1</sup>* allele used in the previous study, which encodes a nearly full-length protein and exhibits similar protein stability as wild-type Ham (Figure 3B; Moore et al., 2002). We took two approaches to determine whether *ham* is required for preventing supernumerary type II neuroblast formation. First, we examined *ham* deficiency heterozygous brains and reproducibly observed a mild supernumerary type II neuroblast phenotype ( $9 \pm 0.9$  per lobe,  $n = 12$  brains) (Figure 3—figure supplement 1A). Second, we knocked down *ham* function by overexpressing a *UAS-RNAi* transgene. We found that knocking down *ham* function also led to a mild but statistically significant increase in type II neuroblasts per lobe ( $9.8 \pm 1.8$ ;  $n = 20$  brains) as compared to control brains ( $8 \pm 0$ ;  $n = 10$  brains) (Figure 3—figure supplement 1B). To confirm that *ham* is indeed required for suppressing supernumerary type II neuroblast formation, we generated two new *ham* alleles, *ham<sup>SK1</sup>* and *ham<sup>SK4</sup>*, by CRISPR-Cas9 (Figure 3B). We characterized the effect of the *ham<sup>SK1</sup>* or *ham<sup>SK4</sup>* allele on Ham protein expression using a specific antibody. We found that *ham<sup>SK1</sup>* or *ham<sup>SK4</sup>* homozygous brains show undetectable Ham protein expression (Figure 3C and D; data not presented). This result strongly suggests that mutant Ham protein encoded by the *ham<sup>SK1</sup>* or *ham<sup>SK4</sup>* allele is unstable, and that these two new *ham* alleles are strongly loss-of-function mutants. We then tested if Ham protein is required for suppressing supernumerary

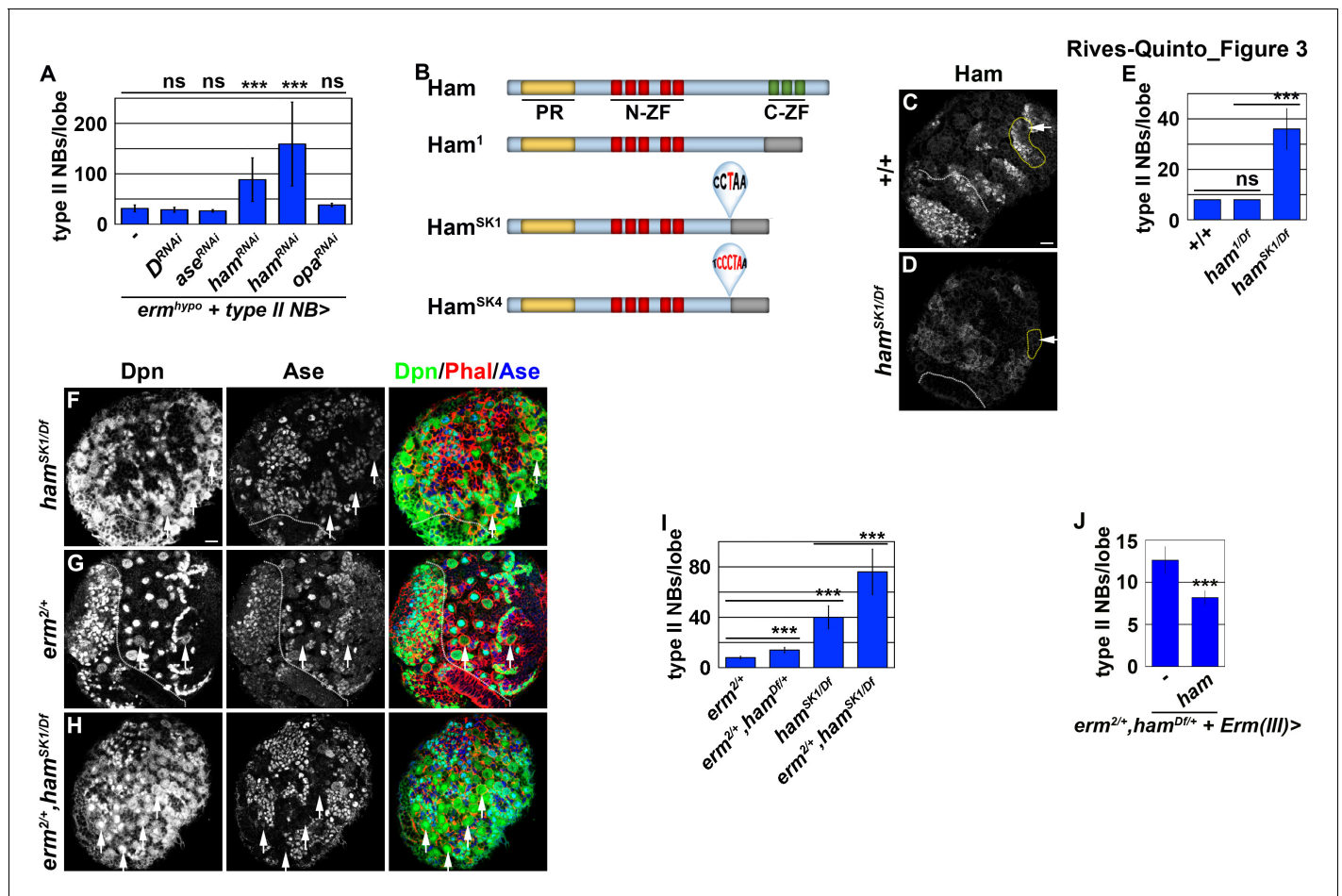


**Figure 3.** Ham is a novel regulator of INP commitment. (A) Quantification of total type II neuroblasts per *erm<sup>hypo</sup>* brain lobe that overexpressed a UAS-RNAi transgene driven by a type II neuroblast Gal4. Knocking-down *ham* function consistently enhanced the supernumerary type II neuroblast phenotype in *erm<sup>hypo</sup>* brains. (B) A diagram summarizing the lesions in *ham* alleles. The molecular lesions in *ham<sup>SK1</sup>* and *ham<sup>SK4</sup>* alleles were not independently verified. (C–D) Ham expression in wild-type or *ham<sup>SK1</sup>* homozygous brains. Ham was detected in immature INPs and INPs in wild-type brains, but was undetectable in *ham<sup>SK1</sup>* homozygous brains. (E) Quantification of total type II neuroblasts per *ham*-mutant brain lobe. *ham<sup>SK1</sup>* homozygous but not *ham<sup>1</sup>* homozygous brains displayed a supernumerary type II neuroblast phenotype. (F–H) Images of *ham* single mutant or *ham*, *erm* double mutant brains. The heterozygosity of *erm* alone had no effect on type II neuroblasts, but enhanced the supernumerary type II neuroblast phenotype in *ham<sup>SK1</sup>* homozygous brains. (I) Quantification of total type II neuroblasts per brain lobe of the indicated genotypes. *erm* and *ham* function synergistically to prevent supernumerary type II neuroblast formation. (J) Quantification of total type II neuroblasts per *erm*,*ham* double heterozygous brain lobe that overexpressed a UAS-*ham* transgene driven by an INP Gal4. Overexpressing Ham in INPs rescued the supernumerary type II neuroblast phenotype in *erm*,*ham* double heterozygous brains. The following labeling applies to all images in this figure: white dashed line separates the optic lobe from the brain; yellow dashed line encircles a type II neuroblast lineage; white arrow: type II neuroblast. Scale bar, 10  $\mu$ m. Bar graphs are represented as mean  $\pm$  standard deviation. p-values: \*\*\*<0.005. ns: not significant.

The online version of this article includes the following source data and figure supplement(s) for figure 3:

**Source data 1.** Quantification of total type II neuroblasts per *erm<sup>hypo</sup>* brain lobe that overexpressed a UAS-RNAi transgene.

**Source data 2.** Quantification of total type II neuroblasts per *ham*-mutant brain lobe.

**Source data 3.** Quantification of total type II neuroblasts per brain lobe of the indicated genotypes.

**Source data 4.** Quantification of total type II neuroblasts per *erm*,*ham* double heterozygous brain lobe that overexpressed a UAS-*ham* transgene.

**Figure supplement 1.** Ham functions synergistically with Erm to suppress supernumerary type II neuroblast formation.

**Figure supplement 1—source data 1.** Quantification of total type II neuroblasts per brain lobe that overexpressed a UAS-*ham<sup>RNAi</sup>* transgene.

type II neuroblast formation. Indeed, *ham<sup>SK1</sup>* homozygous brains contained  $40 \pm 10$  type II neuroblasts per lobe ( $n = 15$  brains) (Figure 3E and F). Because Ham is detectable in *Ase<sup>+</sup>* immature INPs and remains expressed in all INPs (Eroglu et al., 2014), we conclude that *ham* is a novel regulator of INP commitment.

*ham* knock-down drastically enhanced the supernumerary neuroblast phenotype in *erm*<sup>hypo</sup> brains, leading us to hypothesize that *ham* functions together with *erm* to suppress INPs from reverting to supernumerary type II neuroblasts. We tested this hypothesis by examining a potential genetic interaction between *erm* and *ham* during INP commitment. Although the heterozygosity of *erm* did not increase total type II neuroblasts ( $8.1 \pm 0.3$  per lobe;  $n = 11$  brains), it enhanced the supernumerary neuroblast phenotype in *ham* deficiency heterozygous brains and in *ham*<sup>SK1</sup> homozygous brains ( $14 \pm 2.2$  vs.  $76.2 \pm 18.3$  type II neuroblasts per lobe;  $n = 14$  brains per genotype) (**Figure 3G–I**). We conclude that Ham functions synergistically with Erm to suppress supernumerary type II neuroblast formation.

## Ham promotes stable INP commitment by repressing gene transcription

Re-activation of Notch signaling in INPs drives supernumerary type II neuroblast formation in *erm*-null brains (**Weng et al., 2010**). Therefore, we hypothesized that supernumerary type II neuroblasts in *ham*-null brains might also originate from INPs. Whereas *erm,ham* heterozygous brains alone contained  $12.7 \pm 1.6$  type II neuroblasts per lobe ( $n = 9$  brains), overexpressing *ham* in INPs driven by *Erm-Gal4(III)* rescued the supernumerary neuroblast phenotype in *erm,ham* double heterozygous brains ( $8.2 \pm 0.8$  type II neuroblasts per lobe;  $n = 24$  brains) (**Figure 3J**). This result strongly suggests that supernumerary type II neuroblasts originate from INPs in *ham*-null brains. We generated GFP-marked mosaic clones derived from single type II neuroblasts to confirm the origin of supernumerary type II neuroblasts in *ham*-null brains. In wild-type clones ( $n = 9$  clones), the parental type II neuroblast was always surrounded by Ase<sup>-</sup> and Ase<sup>+</sup> immature INPs (**Figure 4A**). By contrast, supernumerary neuroblasts in *ham*<sup>SK1</sup> homozygous clones ( $2.5 \pm 1.7$  type II neuroblasts per clone;  $n = 11$  clones) were always located far away from parental neuroblasts and surrounded by Ase<sup>+</sup> cells that were most likely Ase<sup>+</sup> immature INPs and ganglion mother cells (**Figure 4B and C**). It is highly unlikely that supernumerary neuroblasts in *ham*<sup>SK1</sup> homozygous clones originated from symmetric neuroblast division based on their location relative to parental neuroblasts and the cell types that surround them. Thus, we conclude that Ham suppresses INP reversion to supernumerary type II neuroblasts.

Because Erm suppresses supernumerary type II neuroblast formation by repressing gene transcription, Ham likely prevents INP reversion as a transcriptional repressor. We reasoned that Ham might function through its N-terminal zinc finger to prevent INP reversion based on our finding that *ham*<sup>SK1</sup> but not *ham*<sup>1</sup> homozygous clones displayed a supernumerary neuroblast phenotype (**Figure 4C**). Consistent with this hypothesis, mis-expressing Ham<sup>ΔC-ZF</sup> triggered premature differentiation in type II neuroblasts, identical to mis-expression of full-length Ham ( $n = 10$  brains per genotype) (**Figure 4E**). We tested if overexpressing Ham<sup>ΔC-ZF</sup> in INPs can rescue the supernumerary neuroblast phenotype in *ham*<sup>SK1</sup> homozygous brains by incubating larvae at 33°C for 96 hr. Incubating *ham*<sup>SK1</sup> homozygous larvae at an elevated temperature leads to a severer supernumerary neuroblast phenotype than at 25°C (**Figures 3E and 4F**). Overexpressing Ham<sup>ΔC-ZF</sup> rescued the supernumerary neuroblast phenotype in *ham*<sup>SK1</sup> homozygous brains to a similar extent as overexpressing full-length Ham ( $11.1 \pm 1.4$  vs.  $11.9 \pm 1.3$  type II neuroblasts per lobe;  $n = 11$  or 9 brains, respectively) (**Figure 4F**). Under identical conditions, overexpressing a constitutive transcriptional repressor form of Ham containing only the N-terminal zinc fingers (ERD::Ham<sup>N-ZF</sup>) also rescued the supernumerary neuroblast phenotype in *ham*<sup>SK1</sup> homozygous brains ( $14 \pm 2.3$  type II neuroblasts per lobe;  $n = 9$  brains) (**Figure 4D and F**). These results indicate that Ham functions through the N-terminal zinc finger to repress the transcription of genes that can trigger INP reversion to supernumerary type II neuroblasts.

Finally, we tested if the N-terminal zinc finger of Ham mediates target gene recognition. We mis-expressed a constitutive transcriptional activator form of Ham containing only the N-terminal zinc-finger motif (VP16::Ham<sup>N-ZF</sup>) (**Figure 4D**). We found that VP16::Ham<sup>N-ZF</sup> misexpression in type II neuroblasts was sufficient to induce supernumerary neuroblast formation ( $17.1 \pm 4.7$  type II neuroblasts per lobe;  $n = 10$  brains) (**Figure 4G**). Because VP16::Ham<sup>N-ZF</sup> can exert a dominant-negative effect, we conclude that Ham suppresses INP reversion by recognizing target genes through its N-terminal zinc-finger motif and repressing their transcription.

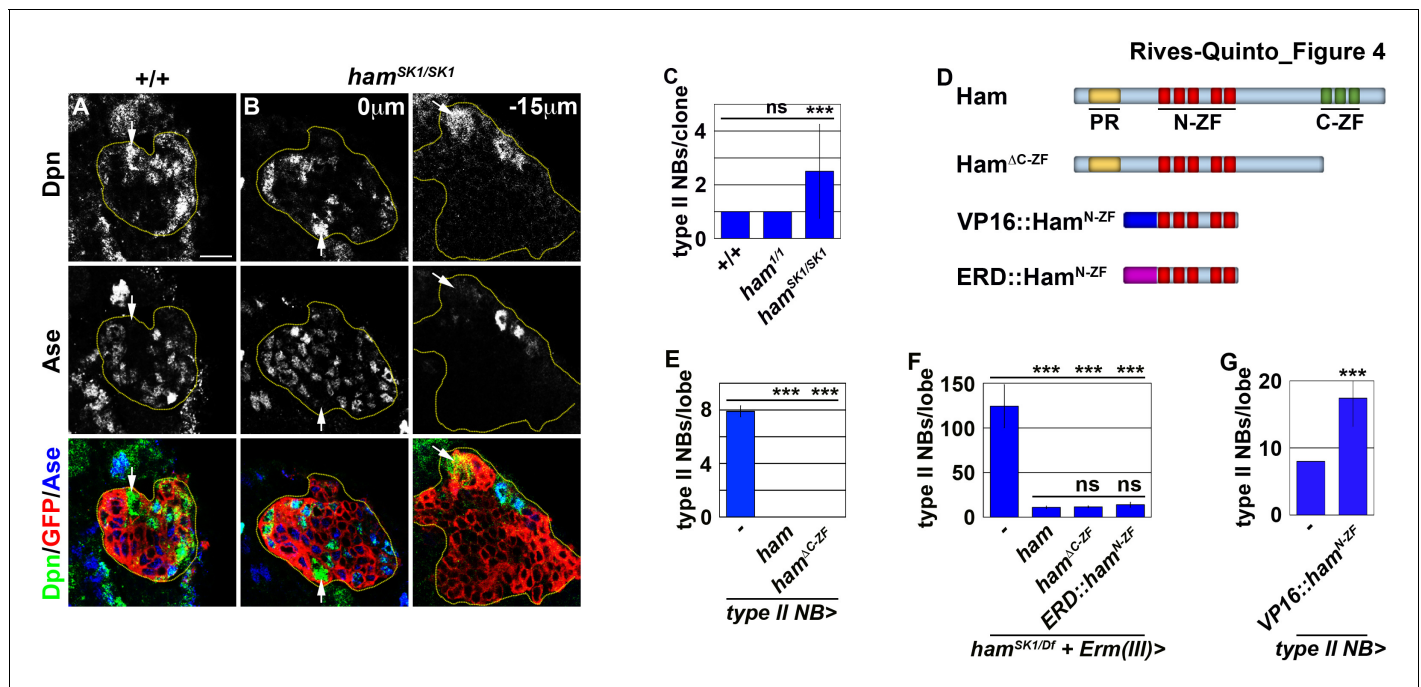


**Figure 4.** Ham suppresses INP reversion by repressing gene transcription. (A–B) Images of wild-type or *ham<sup>SK1</sup>* homozygous type II neuroblast mosaic clones. Supernumerary neuroblasts (–15  $\mu$ m) in *ham<sup>SK1</sup>* homozygous clones were always located far from the parental neuroblast (0  $\mu$ m), and were surrounded by Ase<sup>+</sup> cells. (C) Quantification of total neuroblasts per *ham<sup>+/+</sup>* or *ham<sup>SK1</sup>* homozygous type II neuroblast clone. *ham<sup>SK1</sup>* homozygous clones contained supernumerary neuroblasts but *ham<sup>+/+</sup>* homozygous clones did not. (D) A diagram summarizing UAS-*ham* transgenes used in this study. (E) Quantification of total type II neuroblasts per brain lobe that overexpressed a UAS-*ham* transgene driven by a type II neuroblast Gal4. Overexpressing full-length Ham or Ham<sup>ΔC-ZF</sup> led to premature differentiation in type II neuroblasts. (F) Quantification of total type II neuroblasts per *ham<sup>SK1</sup>* homozygous brain lobe that overexpressed various UAS-*ham* transgenes driven by an INP Gal4. Overexpressed full-length Ham, Ham<sup>ΔC-ZF</sup> or ERD::Ham<sup>N-ZF</sup> rescued the supernumerary neuroblast phenotype in *ham<sup>SK1</sup>* homozygous brains. (G) Quantification of total type II neuroblasts per brain lobe that overexpressed a UAS-VP16::*ham<sup>N-ZF</sup>* transgene driven by a type II neuroblast Gal4. Overexpressing VP16::Ham<sup>N-ZF</sup> led to supernumerary type II neuroblast formation. The following labeling applies to all images in this figure: yellow dashed line encircles a type II neuroblast lineage; white arrow: type II neuroblast. Scale bar, 10  $\mu$ m. Bar graphs are represented as mean  $\pm$  standard deviation. Ppvalues: \*\*\*<0.005. ns: not significant. The online version of this article includes the following source data for figure 4:

**Source data 1.** Quantification of total neuroblasts per *ham<sup>+/+</sup>* or *ham<sup>SK1</sup>* homozygous type II neuroblast clone.

**Source data 2.** Quantification of total type II neuroblasts per brain lobe that overexpressed a UAS-*ham* transgene.

**Source data 3.** Quantification of total type II neuroblasts per *ham<sup>SK1</sup>* homozygous brain lobe that overexpressed various UAS-*ham* transgenes.

**Source data 4.** Quantification of total type II neuroblasts per brain lobe that overexpressed a UAS-VP16::*ham<sup>N-ZF</sup>* transgene.

## Inactivation during INP commitment relinquishes Notch's ability to activate *tll* in INPs

Our findings strongly suggest that Erm and Ham inactivate *tll* during INP commitment, preventing the re-activation of Notch signaling from triggering *tll* expression in INPs (Figure 5A). Therefore, we tested if Erm and Ham indeed inactivate *tll* by reducing *tll* function in *erm,ham* double heterozygous brains. *tll* heterozygous brains contained  $8.2 \pm 0.4$  type II neuroblasts per lobe, whereas *erm,ham* double heterozygous brains contained  $11 \pm 1.2$  type II neuroblasts per lobe ( $n = 10$  or 25 brains, respectively) (Figure 5B). The heterozygosity of *tll* consistently suppressed the supernumerary neuroblast phenotype in *erm,ham* double heterozygous brains ( $8.4 \pm 0.6$  type II neuroblasts per lobe;  $n = 22$  brains) (Figure 5B). This result strongly supports our hypothesis that Erm and Ham inactivate *tll* during INP commitment. Consistent with this interpretation, we found that Tll::GFP becomes ectopically expressed in INPs in *erm,ham* double heterozygous brains (Figure 5C). In these brains, we reproducibly observed small cells expressing Tll::GFP and Deadpan (Dpn) but not Ase that were most likely supernumerary type II neuroblasts newly derived from INP reversion (Figure 5D). Furthermore, we found that one copy of the *tll::GFP(BAC)* transgene mildly enhanced the supernumerary

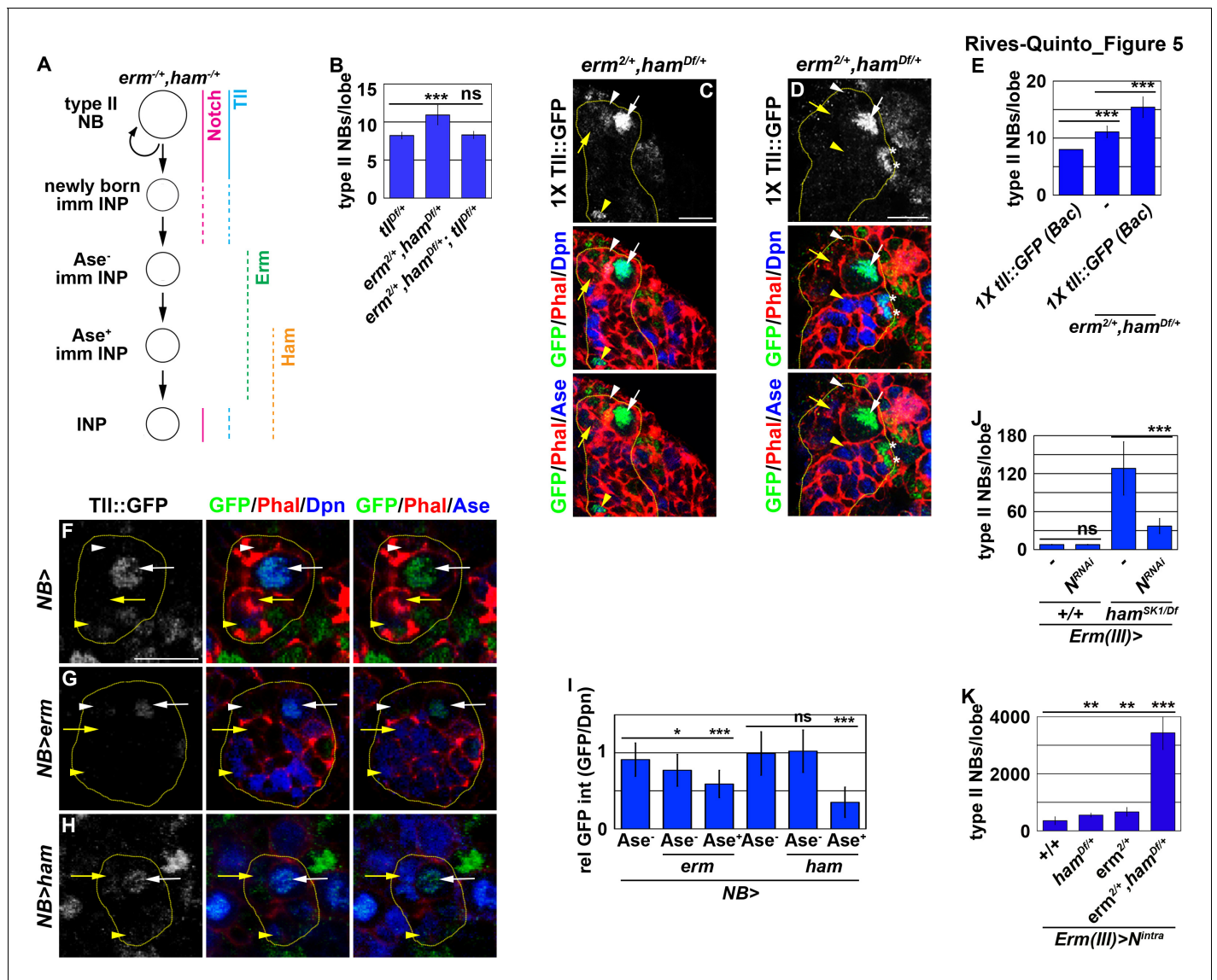


**Figure 5.** Erm- and Ham-mediated repression renders *tll* refractory for activation by Notch. (A) A diagram depicting our hypothesis that ectopic activation of *tll* in INPs leads to supernumerary type II neuroblasts in *erm,ham* double heterozygous brains. (B) Quantification of total type II neuroblasts per brain lobe that was *erm,ham* double heterozygous or *erm,ham,tll* triple heterozygous. Heterozygosity of *tll* suppressed the supernumerary neuroblast phenotype in *erm,ham* double heterozygous brains. (C–D) Images of *erm,ham* double heterozygous brains that carries a *tll::GFP(BAC)* transgene. Tll::GFP becomes ectopically expressed in INPs and supernumerary type II neuroblasts (\*) in *erm,ham* double heterozygous brains. (E) Quantification of total type II neuroblasts *erm,ham* double heterozygous brain lobe that carried one copy of the *tll::GFP(BAC)* transgene. One copy of the *tll::GFP(BAC)* transgene was sufficient to enhance the supernumerary type II neuroblast phenotype in *erm,ham* double heterozygous brains. (F–H) Images of type II neuroblasts that mis-expressed a *UAS-erm* or *UAS-ham* transgene driven by a pan-neuroblast Gal4. Erm or Ham mis-expression drastically reduced Tll::GFP expression in type II neuroblasts. (I) Quantification of Tll::GFP expression relative to Dpn expression in type II neuroblasts that mis-expressed a *UAS-erm* or *UAS-ham* transgene driven by a pan-neuroblast Gal4. Erm mis-expression reduced Tll::GFP expression in type II neuroblasts before the onset of Ase expression, whereas Ham mis-expression reduced Tll::GFP expression in type II neuroblasts after the onset of Ase expression. (J) Quantification of total type II neuroblasts per wild-type or *ham<sup>SK1</sup>* homozygous brain lobe that overexpressed a *UAS-N<sup>RNAi</sup>* transgene driven by an INP Gal4. Knocking-down Notch function in INPs suppressed the supernumerary type II neuroblast phenotype in *ham<sup>SK1</sup>* homozygous brains. (K) Quantification of total type II neuroblasts per *erm* or *ham* heterozygous brain lobe that overexpressed a *UAS-N<sup>intra</sup>* transgene driven by an INP Gal4. Overexpressing *N<sup>intra</sup>* in INPs more efficiently induced supernumerary neuroblasts in *erm,ham* double heterozygous brains than in *erm* or *ham* heterozygous brains. The following labeling is applicable to all panels of images in this figure: yellow dashed line encircles a type II neuroblast lineage; white arrow: type II neuroblast; white arrowhead: Ase<sup>-</sup> immature INP; yellow arrow: Ase<sup>+</sup> immature INP; yellow arrowhead: INP; \*: supernumerary type II neuroblasts. Scale bar, 10 μm. Bar graphs are represented as mean ± standard deviation. p-values: \*\*<0.05, \*\*\*<0.005. ns: not significant. The online version of this article includes the following source data for figure 5:

**Source data 1.** Quantification of total type II neuroblasts per brain lobe that was *erm,ham* double heterozygous or *erm,ham,tll* triple heterozygous.  
**Source data 2.** Quantification of total type II neuroblasts *erm,ham* double heterozygous brain lobe that carried one copy of the *tll::GFP(BAC)* transgene.

**Source data 3.** Quantification of Tll::GFP expression relative to Dpn expression in type II neuroblasts that mis-expressed a *UAS-erm* or *UAS-ham* transgene.

**Source data 4.** Quantification of total type II neuroblasts per wild-type or *ham*<sup>SK1</sup> homozygous brain lobe that overexpressed a *UAS-N<sup>RNAi</sup>* transgene.

**Source data 5.** Quantification of total type II neuroblasts per *erm* or *ham* heterozygous brain lobe that overexpressed a *UAS-N<sup>intra</sup>* transgene.

neuroblast phenotype in *erm,ham* double heterozygous brains ( $15.4 \pm 1.8$  vs.  $11.1 \pm 1$  type II neuroblasts per lobe;  $n = 12$  or  $11$  brains, respectively) (Figure 5E). These data strongly support our model that Erm and Ham inactivate *tll* during INP commitment. We tested this model by overexpressing *erm* or *ham* in type II neuroblasts that carry one copy of the *tll::GFP(Bac)* transgene. We found that Tll::GFP expression in type II neuroblasts overexpressing Erm was mildly reduced prior to upregulation of Ase expression, and declined further following upregulation of Ase expression (Figure 5F, G and I). By contrast, Tll::GFP expression in type II neuroblasts overexpressing Ham was unaffected prior to upregulation of Ase expression, but rapidly declined following upregulation of Ase expression (Figure 5H and I). Together, these data strongly support our model that sequential inactivation by Erm and Ham during INP commitment renders *tll* refractory to activation in INPs.

Because *tll* is a putative target of Notch, we tested if inactivation of *tll* by Erm and Ham relinquishes the ability of Notch signaling to activate *tll* in INPs. We knocked-down Notch function in INPs in wild-type or *ham*<sup>SK1</sup> homozygous brains. Knock-down of Notch function in INPs had no effect on type II neuroblasts in wild-type brains ( $7.9 \pm 0.3$  type II neuroblasts per lobe;  $n = 17$  brains) (Figure 5J). However, in *ham*<sup>SK1</sup> homozygous brains, knocking-down Notch function in INPs reduced the number of type II neuroblasts per lobe from  $128 \pm 39.6$  to  $36.4 \pm 11.6$  ( $n = 9$  brains per genotype) (Figure 5J). This result indicates that re-activation of Notch signaling triggers INP reversion to supernumerary type II neuroblasts in *ham*-null brains. We extended our analyses to test if inactivation by Erm and Ham reduces the competency to respond to Notch signaling. Consistently, overexpressing constitutively activated Notch (Notch<sup>intra</sup>) induced a drastically more severe supernumerary neuroblast phenotype in *erm,ham* double heterozygous brains ( $3,437.6 \pm 586.8$  type II neuroblasts per lobe;  $n = 9$  brains) than in *erm* or *ham* single heterozygous brains ( $687 \pm 134.3$  vs.  $588.6 \pm 77.6$  type II neuroblasts per lobe;  $n = 9$  or  $11$  brains, respectively) (Figure 5K). Thus, we propose that inactivation by Erm and Ham during INP commitment renders *tll* refractory to Notch signaling in INPs (Figure 5A).

### Inactivation by Hdac3 relinquishes Notch's ability to activate *tll* in INPs

To prevent Notch signaling from activating *tll* in INPs, Erm and Ham must function through chromatin-modifying proteins. We first tested if Erm and Ham inactivate *tll* by promoting sequential chromatin changes during INP commitment. We overexpressed full-length Ham or Ham<sup>ΔC-ZF</sup> driven by *Erm-Gal4(III)* in *erm*-null brains. *erm*-null brains alone contained  $1824.6 \pm 520.7$  type II neuroblasts per lobe ( $n = 13$  brains) (Figure 6A and Figure 6—figure supplement 1A). Overexpressing full-length Ham or Ham<sup>ΔC-ZF</sup> strongly suppressed the supernumerary neuroblast phenotype in *erm*-null brains ( $34.5 \pm 8.3$  vs.  $64.6 \pm 18.3$  neuroblasts per lobe;  $n = 13$  or  $7$  brains, respectively) (Figure 6A and Figure 6—figure supplement 1B). This result indicates that Ham over-expression can replace endogenous Erm function to suppress INP reversion, suggesting that these two transcriptional repressors function through an identical chromatin-modifying protein to inactivate *tll* during INP commitment.

We predicted that decreasing the activity of a chromatin-modifying protein required for Ham-mediated gene inactivation during INP commitment should enhance the supernumerary neuroblast phenotype in *ham* heterozygous brains. We knocked-down the function of genes known to contribute to the inactivation of gene transcription in *ham* heterozygous brains. Reducing the activity of PRC2 or heterochromatin protein 1, as well as decreasing the recruitment of Heterochromatin Protein 1, had no effect on the supernumerary neuroblast phenotype in *ham* heterozygous brains (Figure 6B). While reducing the activity of nucleosome remodelers alone led to a mild supernumerary type II neuroblast phenotype, it did not further enhance the supernumerary neuroblast phenotype in *ham* heterozygous brains (Figure 6C). By contrast, reducing the activity of histone deacetylase 3 (Hdac3) alone resulted in a mild supernumerary type II neuroblast phenotype and significantly enhanced the supernumerary neuroblast phenotype in *ham* heterozygous brains (Figure 6C). These results led us to conclude that Ham likely functions through Hdac3 to prevent

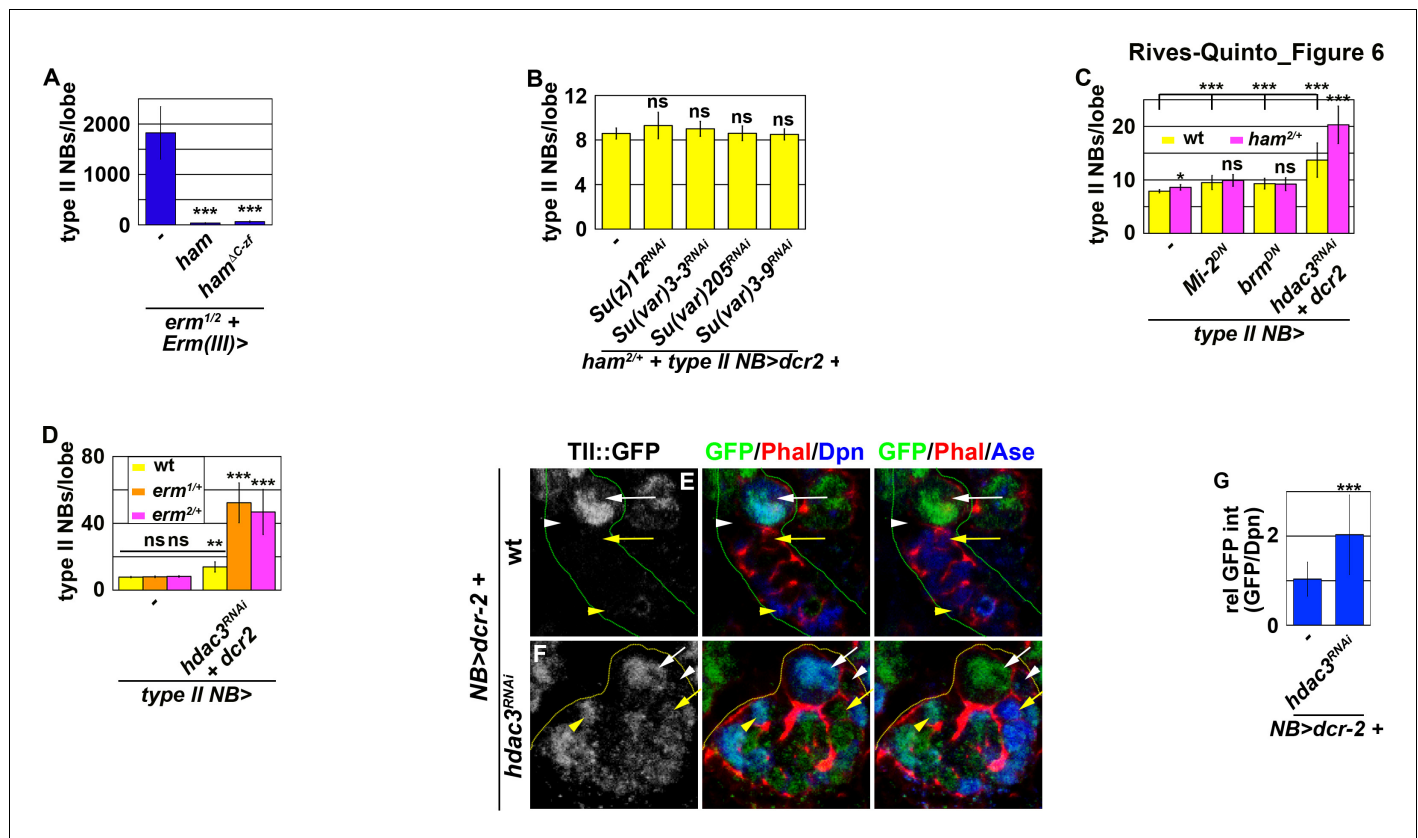


**Figure 6.** Erm and Ham function through Hdac3 to prevent INPs from reverting to type II neuroblasts. (A) Quantification of total type II neuroblasts per brain lobe that overexpressed a *UAS-ham* transgene driven by an INP Gal4. Overexpressing full-length Ham or Ham<sup>ΔC-ZF</sup> in INPs suppressed the supernumerary type II neuroblast phenotype in *erm*-null brains. (B) Quantification of total type II neuroblasts per *ham* heterozygous brain lobe that overexpressed a *UAS-RNAi* transgene driven by a type II neuroblast Gal4. Reducing activity of the indicated chromatin complex did not increase INP reversion into supernumerary type II neuroblasts in *ham* heterozygous brains. (C) Quantification of total type II neuroblasts per *ham* heterozygous brain lobe that overexpressed a *UAS* transgene driven by a type II neuroblast Gal4. Reducing Hdac3 activity increased INP reversion into supernumerary type II neuroblasts in *ham* heterozygous brains. (D) Quantification of total type II neuroblasts per *erm* heterozygous brain lobe that overexpressed a *UAS-hdac3<sup>RNAi</sup>* transgene driven by a type II neuroblast Gal4. Reducing Hdac3 activity increased INP reversion into supernumerary type II neuroblasts in *erm* heterozygous brains. (E–F) Images of *tll::GFP(Bac)* brains that overexpressed a *UAS-hdac3<sup>RNAi</sup>* transgene driven by a pan-neuroblast Gal4. Reducing Hdac3 activity in type II neuroblasts led to ectopic *Tll::GFP* expression in immature INPs and INPs. (G) Quantification of *Tll::GFP* expression relative to Dpn expression in INPs derived from type II neuroblasts that overexpressed a *UAS-hdac3<sup>RNAi</sup>* transgene. Reducing Hdac3 activity in type II neuroblasts led to ectopic *Tll::GFP* expression in INPs. The following labeling is applicable to all panels of images in this figure: yellow dashed line encircles a type II neuroblast lineage; white arrow: type II neuroblast; white arrowhead: Ase<sup>-</sup> immature INP; yellow arrow: Ase<sup>+</sup> immature INP; yellow arrowhead: INP. Bar graphs are represented as mean ± standard deviation. p-values: \*\*<0.05, \*\*\*<0.005. ns: not significant.

The online version of this article includes the following source data and figure supplement(s) for figure 6:

**Source data 1.** Quantification of total type II neuroblasts per brain lobe that overexpressed a *UAS-ham* transgene.

**Source data 2.** Quantification of total type II neuroblasts per *ham* heterozygous brain lobe that overexpressed various *UAS* transgenes.

**Source data 3.** Quantification of total type II neuroblasts per *erm* heterozygous brain lobe that overexpressed a *UAS-hdac3<sup>RNAi</sup>* transgene.

**Source data 4.** Quantification of *Tll::GFP* expression relative to Dpn expression in INPs derived from type II neuroblasts that overexpressed a *UAS-hdac3<sup>RNAi</sup>* transgene.

**Figure supplement 1.** Ham overexpression in Ase<sup>+</sup> immature INPs suppressed INP reversion in *erm*-null brains.

INP reversion. We next tested if Erm also functions through Hdac3 to prevent INP reversion. *erm* heterozygous brains alone did not display a supernumerary type II neuroblast phenotype (Figure 6D). Knocking-down *hdac3* function in *erm* heterozygous brains led to a more than three-fold increase in supernumerary type II neuroblasts as compared to wild-type brains (Figure 6D). These data strongly support a model that Hdac3 functions together with Erm and Ham to silence *tll* during INP commitment.

We tested if *hdac3* is indeed required for silencing *tll* during INP commitment by overexpressing a *UAS-hdac3<sup>RNAi</sup>* transgene in type II neuroblasts. Consistent with our hypothesis, knock down of *hdac3* function in type II neuroblasts and their progeny led to ectopic Tll::GFP expression in immature INPs and INPs (**Figure 6E–G**). These results confirmed that Hdac3 is required for inactivating *tll* during INP commitment. Thus, we conclude that Erm and Ham likely function through Hdac3 to prevent INP from reverting to supernumerary type II neuroblasts by continually inactivating *tll*.

## Discussion

The expansion of OSVZ neural stem cells, which indirectly produce neurons by initially generating intermediate progenitors, drives the evolution of lissencephalic brains to gyrencephalic brains (Cárdenas and Borrell, 2020; Delaunay et al., 2017; Di Lullo and Kriegstein, 2017). Recent studies have revealed important insights into genes and cell biological changes that lead to the formation of OSVZ neural stem cells (Fujita et al., 2020; Namba et al., 2020). However, the mechanisms controlling the functional identity of OSVZ neural stem cells, including the competency to generate intermediate progenitors, remain unknown. In this study, we have provided compelling evidence demonstrating that Tll is necessary and sufficient for the maintenance of an undifferentiated state and the competency to generate intermediate progenitors in type II neuroblasts (**Figure 7**). We also showed that two sequentially activated transcriptional repressors, Erm and Ham, likely function through Hdac3 to silence *tll* during INP commitment ensuring normal indirect neurogenesis in larval brains. We propose that continual inactivation of stem cell functional identity genes by histone deacetylation allows intermediate progenitors to stably commit to generating sufficient and diverse differentiated cells during neurogenesis.

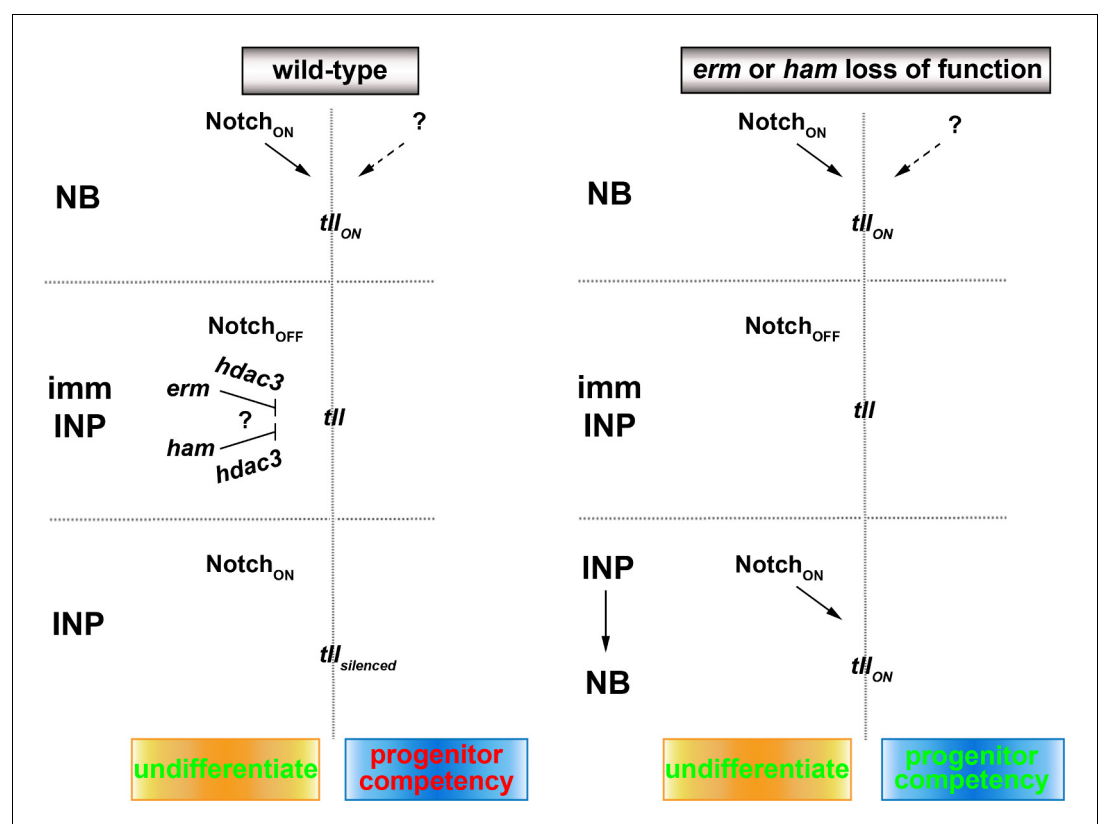


**Figure 7.** A proposed model for the regulation of type II neuroblast functionality. We propose that Erm and Ham recruits Hdac3 to silence *tll* during INP commitment, preventing re-activation of Notch signaling in INPs from triggering Tll expression in wild-type brains. The *tll* locus remains in an activatable state in *erm*- or *ham*-null brains, and re-activation of Notch signaling in INPs triggers aberrant Tll expression driving INP reversion to supernumerary type II neuroblasts.

## Regulation of the maintenance of an undifferentiated state and the competency to generate intermediate progenitors in neural stem cells

Stem cell functional identities encompass the maintenance of an undifferentiated state and other unique functional features, such as the competency to generate intermediate progenitors. Because genetic manipulation of Notch signaling perturbs the regulation of differentiation during asymmetric stem cell division (Imayoshi et al., 2010; Kageyama et al., 2008), the role of Notch in regulating other stem cell functions remains poorly understood. In the fly type II neuroblast lineage, overexpressing Notch<sup>intra</sup> or the downstream transcriptional repressors Dpn, E(spl)my, and Klumpfuss (Klu) induces the formation of supernumerary type II neuroblasts at the expense of generating immature INPs via the inhibition of *erm* activation (Janssens et al., 2017). These results indicate that the Notch-Dpn/E(spl)my/Klu axis provides an evolutionarily conserved mechanism to maintain neural stem cells in an undifferentiated state. Although overexpressing Notch<sup>intra</sup> but not Dpn, E(spl)my, and Klu in combination in INPs is sufficient to drive supernumerary type II neuroblast formation, Notch<sup>intra</sup> overexpression is not sufficient to transform a type I neuroblast into a type II neuroblast (data not presented). Thus, we propose that Notch functions as a general activator of genes expression in type II neuroblasts, and specific regulators of type II neuroblast functional identities must exist.

Our study strongly suggests that *tll* functions as a master regulator of type II neuroblast functional identities (Figure 7). Identical to *Notch*, *tll* is necessary for maintaining type II neuroblasts in an undifferentiated state and is sufficient to induce INP reversion into type II neuroblasts (Figure 2B–G; Hakes and Brand, 2020). Uniquely, high levels of Tll is sufficient to molecularly transform greater than 60% of type I neuroblasts in the ventral brain region into type II neuroblasts (Figure 2H–M). Brain regionalization leads to distinct degrees of sensitivity to Tll overexpression. For example, type I neuroblasts in the dorsal-anterior region of the brain are resistant to Tll-induced lineage transformation. By contrast, Tll overexpression can transform most, if not all, type I neuroblasts in the ventral-lateral and ventral-medial regions of the brain into type II neuroblasts. High levels of Tll expression in ventral-lateral type I neuroblasts leads to accumulation of mostly supernumerary type II neuroblasts and very few Erm::V5<sup>+</sup> immature INPs. This result phenocopies Tll overexpression driven by strong drivers in the type II neuroblast lineages, and suggests that neuroblast progeny rapidly reacquire a neuroblast identity instead of an immature INP identity (data not presented) (Hakes and Brand, 2020). Tll overexpression in ventral-medial type I neuroblasts leads to the formation of supernumerary type II neuroblasts interspersed with Erm::V5<sup>+</sup> immature INPs, mimicking Tll overexpression driven by moderate drivers in the type II neuroblast lineages. We speculate that progeny of transformed type II neuroblasts in the ventral-medial region of the brain can assume an immature INP identity and then revert into supernumerary type II neuroblasts. These data strongly support a model that Tll is a potent activator of type II neuroblast functional identities.

A key question regarding the proposed function of Tll in regulating type II neuroblast functional identities is how it mechanistically links to genes previously shown to control these characteristics. ChIP-seq on fly embryonic nuclear extract using the Tll::GFP(Bac) transgenic protein identified hundreds of putative Tll target genes that include all previously characterized regulators of type II neuroblast functional identities (Davis et al., 2018). Tll binds *dpn*, *E(spl)my* and *klu* loci in embryos, suggesting that Tll likely regulates their expression. The phenotypic effects of loss- and gain-of-function of *tll* on type II neuroblasts mimic those of *dpn*, *E(spl)my* and *klu*. The vertebrate homolog of Tll, Tlx, has been shown to function as a transcriptional activator during neurogenesis (Sun et al., 2017). Thus, Tll might maintain type II neuroblasts in an undifferentiated state by promoting *dpn*, *E(spl)my* and *klu* expression. Tll also binds *pntP1* and *btd* loci in embryos. Similar to Tll overexpression, mis-expression of *PntP1* or *Btd* can transform type I neuroblasts in the ventral brain region into type II neuroblasts (Komori et al., 2014b; Xie et al., 2014; Zhu et al., 2011). Thus, it is plausible that *tll* functions through *pntP1* or *btd* to regulate the competency to generate INPs in type II neuroblasts. These results strongly support our model that Tll is key component of the regulatory mechanism that endows type II neuroblasts with lineage-specific functional identities. Future experiments to validate the mechanistic links between *tll* and genes that regulate various lineage-specific functional characteristics will allow for the establishment of gene regulatory circuits that regulate type II neuroblast functional identities.

## Successive transcriptional repressor activity inactivates stem cell functional identity genes during progenitor commitment

The identification of *ham* as a putative regulator of INP commitment was unexpected given that a previously published study concluded that Ham functions to limit INP proliferation (Eroglu et al., 2014). Ham is the fly homolog of Prdm16 in vertebrates and has been shown to play a key role in regulating cell fate decisions in multiple stem cell lineages (Baizabal et al., 2018; Harms et al., 2015; Moore et al., 2002; Shimada et al., 2017). Prdm16 contains two separately defined zinc-finger motifs, with each likely recognizing unique target genes. Prdm16 can also function through a variety of cofactors to activate or repress target gene expression, independent of its DNA-binding capacity. Thus, Ham can potentially inactivate stem cell functionality genes via one of several mechanisms. By using a combination of previously isolated alleles and new protein-null alleles, we demonstrated that the N-terminal zinc-finger motif is required for Ham function in immature INPs. Based on the overexpression of a series of chimeric proteins containing the N-terminal zinc-finger motif, our data indicate that Ham prevents INP reversion to supernumerary type II neuroblasts by recognizing target genes via the N-terminal zinc-finger motif and possibly repressing their transcription. Our results suggest that Ham prevents INPs from reverting to supernumerary type II neuroblasts by possibly repressing target gene transcription.

A key question raised by our study is why two transcriptional repressors that seemingly function in a redundant manner are required to prevent INPs from reverting to supernumerary type II neuroblasts. INP commitment lasts approximately 6–8 hr following the generation of an immature INP (Berger et al., 2012; Homem et al., 2014); after this time, the immature INP transitions into an INP. *erm* is poised for activation in type II neuroblasts and becomes rapidly activated in the newly generated immature INP less than 90 min after its generation (Janssens et al., 2017). As such, Erm-mediated transcriptional repression allows for the rapid inactivation of type II neuroblast functional identity genes. Because Erm expression rapidly declines in INPs when Notch signaling becomes reactivated, a second transcriptional repressor that becomes activated after Erm and whose expression is maintained throughout the life of an INP is required to continually inactivate type II neuroblast functional identity genes. Ham is an excellent candidate because it becomes expressed in immature INPs 3–4 hr after the onset of Erm expression and is detected in all INPs. Similar to Erm, Ham recognizes target genes and represses their transcription. Furthermore, *ham* functions synergistically with *erm* to prevent INP reversion to supernumerary type II neuroblasts, and overexpressed Ham can partially substitute for endogenous Erm. Thus, Erm- and Ham-mediated transcriptional repression renders type II neuroblast functional identity genes refractory to activation by Notch signaling throughout the lifespan of the INP, ensuring the generation of differentiated cell types rather than supernumerary type II neuroblasts instead.

## Sustained inactivation of stem cell functional identity genes distinguishes intermediate progenitors from stem cells

Genes that specify stem cell functional identity become refractory to activation during differentiation, but the mechanisms that restrict their expression are poorly understood due to a lack of lineage information. Researchers have proposed several epigenetic regulator complexes that may restrict neural stem-cell-specific gene expression in neurons (Hirabayashi and Gotoh, 2010; Ronan et al., 2013). We knocked-down the function of genes that were implicated in restricting neural stem cell gene expression during differentiation in order to identify chromatin regulators that are required to inactivate type II neuroblast functional identity genes during INP commitment. Surprisingly, we found that only Hdac3 is required for both Erm- and Ham-mediated suppression of INP reversion to type II neuroblasts. Our finding is consistent with a recent study showing that blocking apoptosis in lineage clones derived from PRC2-mutant type II neuroblasts did not lead to supernumerary neuroblast formation (Abdusselamoglu et al., 2019). Our data strongly suggest that genes specifying type II neuroblast functional identity, such as *tll*, are likely silenced rather than decommissioned in INPs. This result is supported by the finding that overexpressing Notch<sup>intra</sup> but not Notch downstream transcriptional repressors in INPs can re-establish a type II neuroblast-like undifferentiated state. We speculate that continual histone deacetylation is required to counter the transcriptional activator activity of endogenous Notch and silence *tll* in INPs (Figure 7). By contrast, the chromatin in the *tll* locus might be close and inaccessible to the Notch transcriptional activator complex in type

I neuroblasts; thus, overexpressing Notch<sup>intra</sup> cannot transform type I neuroblasts into type II neuroblasts. A key remaining question is what transcription factor is required to maintain the chromatin in the *tll* loci in an open state. Insights into regulation of the competency of the *tll* locus to respond to activated Notch signaling might improve our understanding of the molecular determinants of OSVZ neural stem cells.

## Materials and methods

### Fly genetics and transgenes

Fly crosses were carried out in 6-oz plastic bottles, and eggs were collected on apple caps in 8 hr intervals. Newly hatched larvae were genotyped and allowed to grow on corn meal caps. Larvae were shifted to 33°C for 72 hr to induce UAS-transgene expression for overexpression or knock down studies prior to dissection.

Larvae for MARCM analyses were genotyped at hatching and allowed to grow at 25°C for 24 hr. Larvae were then shifted to a 37°C water bath for 90 min to induce clones. Heat-shocked larvae were allowed to recover and grow at 25°C for 72 hr prior to dissection.

Transgenes were inserted into the *pUAST-attB M{3xP3-RFP.attP}ZH-86Fb* docking site using  $\Phi$ C31 integrase-mediated transgenesis (Bischof and Basler, 2008). DNA injections were carried out by BestGene Inc or Genetivision Inc, and transgenic flies were identified in the F1 generation based on their red eye color.

### Immunofluorescent staining and antibodies

Larval brains were dissected in PBS and fixed in 100 mM PIPES (pH 6.9), 1 mM EGTA, 0.3% Triton X-100, and 1 mM MgSO<sub>4</sub> containing 4% formaldehyde for 23 min. Fixed brain samples were washed with PBST (1XPBS and 0.3% Triton X-100). After removing the fix solution, samples were incubated with primary antibodies for 3 hr at room temperature. Three hours later, samples were washed with PBST and then incubated with secondary antibodies overnight at 4°C. On the next day, samples were washed with PBST and then equilibrated in ProLong Gold antifade mountant (ThermoFisher Scientific). The confocal images were acquired on a Leica SP5 scanning confocal microscope (Leica Microsystems, Inc). More than 10 brains per genotype were used to obtain data in each experiment.

### RNA extraction and qRT-PCR

Total RNA was extracted from control or treated *brat*<sup>11/Df(2L)Exel8040</sup> larvae carrying *2xTub-Gal80<sup>ts</sup>*, *Wor-Gal4* and *UAS-insb* transgenes using TRIzol (ThermoFisher Scientific) and mRNA was purified using the RNeasy Micro Kit (Qiagen) according to the manufacturer's protocol. First strand cDNA was synthesized using a 1<sup>st</sup> Strand cDNA Synthesis Kit for RT-PCR [AMV] (Roche) according to the manufacturer's protocol. cDNA is amplified by using gene-specific primers. qRT-PCR was performed using Absolute QPCR SYBR Green ROX Mix (ThermoFisher Scientific). Data were analyzed by comparative CT method, and the relative mRNA expression was presented.

### Sample preparation and RNA sequencing

Control or treated *brat*<sup>11/Df(2L)Exel8040</sup> larvae carrying *2xTub-Gal80<sup>ts</sup>*, *Wor-Gal4* and *UAS-insb* transgenes were cultured in corn meal caps. One third of the larvae (18 hr Insb OE sample) were allowed to grow at 25°C for 102 hr and then transferred to 33°C to induce transient Insb overexpression for 18 hr. One-third of the larvae (9 hr Insb OE sample) were allowed to grow at 25°C for 111 hr and then transferred to 33°C to induce transient Insb overexpression for 9 hr. The remaining third of the larvae (0 hr Insb OE) were allowed to grow at 25°C for 120 hr. Fifty brains from each group were isolated on the same day, and immediately processed for RNA extraction. Biological triplicate brain samples were collected. Paired-end Poly-A-mRNA libraries were generated to be assayed by Illumina HiSeq 4000. Differential genes expression was based on absolute linear fold change >or equal 1.5.

### Bioinformatics: RNA-seq analysis

Biological triplicate brain samples for each time point were sequenced using Illumina HiSeq 4000. The samples had around 46, 45 and 44 million reads. Quality of the raw reads for each sample was

checked using FastQC (<http://www.bioinformatics.bbsrc.ac.uk/projects/fastqc>). We align the reads to the dm6 reference genome including mRNAs (<http://www.genome.ucsu.edu/>) with HISAT2 (version 2.1.0) and default parameters. Alignment results were validated through a second round of FASTQ followed by quantification and analysis. For differential expression analysis, Stringtie (version 1.3.4) quantifies expression at the gene and isoforms levels and DESeq2 (version 1.20.0) performs differential expression testing. We compared transcriptional profile between 0 hr vs 9 hr, 0 hr vs 18 hr, and 9 hr vs 18 hr. We identified genes and transcripts as being differentially expressed based on absolute linear fold change  $\geq$  1.5.

## Quantification and statistical analysis

The Image J software was used to quantify the number of cells of interest. Dpn single-channel confocal images were used to assign the area the type II Neuroblasts or INP nucleus. All biological replicates were independently collected and processed. All statistical analyses were performed using a two-tailed Student's T-test, a p-value  $< 0.05$ ,  $< 0.005$ , and  $< 0.0005$  were indicated by (\*), (\*\*), and (\*\*\*), respectively in figures.

## Acknowledgements

We thank Drs. E Lai and J Knoblich for providing us with reagents. We thank the Advance Genomics Core and Bioinformatics Core for technical assistance. We thank Dr. Melissa Harrison, Ms. Elizabeth Lawson, and members of the Lee lab for helpful discussions, and Science Editors Network for editing the manuscript. We thank the Bloomington *Drosophila* Stock Center, FlyORF, and the Vienna *Drosophila* RNAi Center for fly stocks. We thank BestGene Inc and GenetiVision for generating the transgenic fly lines. This work is supported by NIH grants R01NS107496 and R01NS111647.

## Additional information

### Funding

Funder	Grant reference number	Author
National Institute of Neurological Disorders and Stroke	R01NS107496	Hideyuki Komori Cheng-Yu Lee
National Institute of Neurological Disorders and Stroke	R01NS111647	Hideyuki Komori Cheng-Yu Lee

The funders had no role in study design, data collection and interpretation, or the decision to submit the work for publication.

### Author contributions

Noemi Rives-Quinto, Hideyuki Komori, Data curation, Formal analysis, Investigation, Methodology, Writing - original draft; Cyrina M Ostgaard, Data curation, Formal analysis, Investigation; Derek H Janssens, Data curation, Formal analysis, Investigation, Methodology; Shu Kondo, Formal analysis, Investigation, Methodology; Qi Dai, Methodology; Adrian W Moore, Cheng-Yu Lee, Conceptualization, Data curation, Formal analysis, Supervision, Funding acquisition, Investigation, Methodology, Writing - original draft, Project administration, Writing - review and editing

### Author ORCIDs

Hideyuki Komori  <https://orcid.org/0000-0001-9764-5654>

Shu Kondo  <http://orcid.org/0000-0002-4625-8379>

Cheng-Yu Lee  <https://orcid.org/0000-0003-2291-1297>

### Decision letter and Author response

Decision letter <https://doi.org/10.7554/eLife.56187.sa1>

Author response <https://doi.org/10.7554/eLife.56187.sa2>

## Additional files

### Supplementary files

- Transparent reporting form

### Data availability

Sequencing data have been deposited in GEO under accession codes GSE152636.

The following dataset was generated:

Author(s)	Year	Dataset title	Dataset URL	Database and Identifier
Rives-Quinto N, Komori H, Lee CY	2020	Sequential activation of transcriptional repressors promotes progenitor commitment by silencing stem cell identity genes	<a href="https://www.ncbi.nlm.nih.gov/geo/query/acc.cgi?acc=GSE152636">https://www.ncbi.nlm.nih.gov/geo/query/acc.cgi?acc=GSE152636</a>	NCBI Gene Expression Omnibus, GSE152636

## References

- Abdusalamoglu MD**, Landskron L, Bowman SK, Eroglu E, Burkard T, Kingston RE, Knoblich JA. 2019. Dynamics of activating and repressive histone modifications in *Drosophila* neural stem cell lineages and brain tumors. *Development* **146**:dev183400. DOI: <https://doi.org/10.1242/dev.183400>, PMID: 31748204
- Baizabal JM**, Mistry M, García MT, Gómez N, Olukoya O, Tran D, Johnson MB, Walsh CA, Harwell CC. 2018. The epigenetic state of PRDM16-Regulated enhancers in radial Glia controls cortical neuron position. *Neuron* **98**: 945–962. DOI: <https://doi.org/10.1016/j.neuron.2018.04.033>, PMID: 29779941
- Bayraktar OA**, Doe CQ. 2013. Combinatorial temporal patterning in progenitors expands neural diversity. *Nature* **498**:449–455. DOI: <https://doi.org/10.1038/nature12266>, PMID: 23783519
- Bello B**, Reichert H, Hirth F. 2006. The brain tumor gene negatively regulates neural progenitor cell proliferation in the larval central brain of *Drosophila*. *Development* **133**:2639–2648. DOI: <https://doi.org/10.1242/dev.02429>, PMID: 16774999
- Bello BC**, Izergina N, Caussinus E, Reichert H. 2008. Amplification of neural stem cell proliferation by intermediate progenitor cells in *Drosophila* brain development. *Neural Development* **3**:5. DOI: <https://doi.org/10.1186/1749-8104-3-5>, PMID: 18284664
- Berger C**, Harzer H, Burkard TR, Steinmann J, van der Horst S, Laurenson AS, Novatchkova M, Reichert H, Knoblich JA. 2012. FACS purification and transcriptome analysis of *Drosophila* neural stem cells reveals a role for klumpfuss in self-renewal. *Cell Reports* **2**:407–418. DOI: <https://doi.org/10.1016/j.celrep.2012.07.008>, PMID: 22884370
- Betschinger J**, Mechtler K, Knoblich JA. 2006. Asymmetric segregation of the tumor suppressor brat regulates self-renewal in *Drosophila* neural stem cells. *Cell* **124**:1241–1253. DOI: <https://doi.org/10.1016/j.cell.2006.01.038>, PMID: 16564014
- Bischof J**, Basler K. 2008. Recombinases and their use in gene activation, gene inactivation, and transgenesis. *Methods Mol Biol* **420**:175–195. DOI: [https://doi.org/10.1007/978-1-59745-583-1\\_10](https://doi.org/10.1007/978-1-59745-583-1_10)
- Boone JQ**, Doe CQ. 2008. Identification of *Drosophila* type II neuroblast lineages containing transit amplifying ganglion mother cells. *Developmental Neurobiology* **68**:1185–1195. DOI: <https://doi.org/10.1002/dneu.20648>, PMID: 18548484
- Bowman SK**, Rolland V, Betschinger J, Kinsey KA, Emery G, Knoblich JA. 2008. The tumor suppressors brat and numb regulate Transit-Amplifying neuroblast lineages in *Drosophila*. *Developmental Cell* **14**:535–546. DOI: <https://doi.org/10.1016/j.devcel.2008.03.004>
- Cárdenas A**, Borrell V. 2020. Molecular and cellular evolution of corticogenesis in amniotes. *Cellular and Molecular Life Sciences* **77**:1435–1460. DOI: <https://doi.org/10.1007/s00018-019-03315-x>, PMID: 31563997
- Davis CA**, Hitz BC, Sloan CA, Chan ET, Davidson JM, Gabdank I, Hilton JA, Jain K, Baymuradov UK, Narayanan AK, Onate KC, Graham K, Miyasato SR, Dreszer TR, Strattan JS, Jolanki O, Tanaka FY, Cherry JM. 2018. The encyclopedia of DNA elements (ENCODE): data portal update. *Nucleic Acids Research* **46**:D794–D801. DOI: <https://doi.org/10.1093/nar/gkx1081>, PMID: 29126249
- Delaunay D**, Kawaguchi A, Dehay C, Matsuzaki F. 2017. Division modes and physical asymmetry in cerebral cortex progenitors. *Current Opinion in Neurobiology* **42**:75–83. DOI: <https://doi.org/10.1016/j.conb.2016.11.009>, PMID: 27978481
- Di Lullo E**, Kriegstein AR. 2017. The use of brain organoids to investigate neural development and disease. *Nature Reviews Neuroscience* **18**:573–584. DOI: <https://doi.org/10.1038/nrn.2017.107>, PMID: 28878372
- Eroglu E**, Burkard TR, Jiang Y, Saini N, Homem CC, Reichert H, Knoblich JA. 2014. SWI/SNF complex regulates prdm protein hamlet to ensure lineage directionality in *Drosophila* neural stem cells. *Cell* **156**:1259–1273. DOI: <https://doi.org/10.1016/j.cell.2014.01.053>
- Farnsworth DR**, Doe CQ. 2017. Opportunities lost and gained: changes in progenitor competence during nervous system development. *Neurogenesis* **4**:e1324260. DOI: <https://doi.org/10.1080/23262133.2017.1324260>, PMID: 28656157

- Fujita I**, Shitamukai A, Kusumoto F, Mase S, Suetsugu T, Omori A, Kato K, Abe T, Shioi G, Konno D, Matsuzaki F. 2020. Endfoot regeneration restricts radial glial state and prevents translocation into the outer subventricular zone in early mammalian brain development. *Nature Cell Biology* **22**:26–37. DOI: <https://doi.org/10.1038/s41556-019-0436-9>, PMID: 31871317
- Hakes AE**, Brand AH. 2020. Tailless/TLX reverts intermediate neural progenitors to stem cells driving tumorigenesis via repression of *asense/ASCL1*. *eLife* **9**:e53377. DOI: <https://doi.org/10.7554/eLife.53377>, PMID: 32073402
- Harms MJ**, Lim HW, Ho Y, Shapira SN, Ishibashi J, Rajakumari S, Steger DJ, Lazar MA, Won KJ, Seale P. 2015. PRDM16 binds MED1 and controls chromatin architecture to determine a Brown fat transcriptional program. *Genes & Development* **29**:298–307. DOI: <https://doi.org/10.1101/gad.252734.114>, PMID: 25644604
- Herr A**, Mckenzie L, Suryadinata R, Sadowski M, Parsons LM, Sarcevic B, Richardson HE. 2010. Geminin and brahma act antagonistically to regulate EGFR-Ras-MAPK signaling in *Drosophila*. *Developmental Biology* **344**:36–51. DOI: <https://doi.org/10.1016/j.ydbio.2010.04.006>, PMID: 20416294
- Hirabayashi Y**, Gotoh Y. 2010. Epigenetic control of neural precursor cell fate during development. *Nature Reviews Neuroscience* **11**:377–388. DOI: <https://doi.org/10.1038/nrn2810>, PMID: 20485363
- Hirata T**, Nakazawa M, Muraoka O, Nakayama R, Suda Y, Hibi M. 2006. Zinc-finger genes *fez* and *Fez*-like function in the establishment of diencephalon subdivisions. *Development* **133**:3993–4004. DOI: <https://doi.org/10.1242/dev.02585>, PMID: 16971467
- Homem CCF**, Reichardt I, Berger C, Lendl T, Knoblich JA. 2014. Long-Term live cell imaging and automated 4D analysis of *Drosophila* neuroblast lineages. *PLOS ONE* **8**:e79588. DOI: <https://doi.org/10.1371/journal.pone.0079588>
- Homem CC**, Repic M, Knoblich JA. 2015. Proliferation control in neural stem and progenitor cells. *Nature Reviews Neuroscience* **16**:647–659. DOI: <https://doi.org/10.1038/nrn4021>, PMID: 26420377
- Imayoshi I**, Sakamoto M, Yamaguchi M, Mori K, Kageyama R. 2010. Essential roles of notch signaling in maintenance of neural stem cells in developing and adult brains. *Journal of Neuroscience* **30**:3489–3498. DOI: <https://doi.org/10.1523/JNEUROSCI.4987-09.2010>, PMID: 20203209
- Janssens DH**, Komori H, Grbac D, Chen K, Koe CT, Wang H, Lee CY. 2014. Earmuff restricts progenitor cell potential by attenuating the competence to respond to self-renewal factors. *Development* **141**:1036–1046. DOI: <https://doi.org/10.1242/dev.106534>, PMID: 24550111
- Janssens DH**, Hamm DC, Anhezini L, Xiao Q, Siller KH, Siegrist SE, Harrison MM, Lee CY. 2017. An Hdac1/Rpd3-Poised circuit balances continual Self-Renewal and rapid restriction of developmental potential during asymmetric stem cell division. *Developmental Cell* **40**:367–380. DOI: <https://doi.org/10.1016/j.devcel.2017.01.014>, PMID: 28245922
- Janssens DH**, Lee CY. 2014. It takes two to tango, a dance between the cells of origin and Cancer stem cells in the *Drosophila* larval brain. *Seminars in Cell & Developmental Biology* **28**:63–69. DOI: <https://doi.org/10.1016/j.semcdb.2014.03.006>, PMID: 24631354
- Kageyama R**, Ohtsuka T, Shimojo H, Imayoshi I. 2008. Dynamic Notch signaling in neural progenitor cells and a revised view of lateral inhibition. *Nature Neuroscience* **11**:1247–1251. DOI: <https://doi.org/10.1038/nn.2208>
- Koe CT**, Li S, Rossi F, Wong JJ, Wang Y, Zhang Z, Chen K, Aw SS, Richardson HE, Robson P, Sung WK, Yu F, Gonzalez C, Wang H. 2014. The Brm-HDAC3-Erm repressor complex suppresses dedifferentiation in *Drosophila* type II neuroblast lineages. *eLife* **3**:e01906. DOI: <https://doi.org/10.7554/eLife.01906>, PMID: 24618901
- Komori H**, Xiao Q, McCartney BM, Lee CY. 2014a. Brain tumor specifies intermediate progenitor cell identity by attenuating  $\beta$ -catenin/Armadillo activity. *Development* **141**:51–62. DOI: <https://doi.org/10.1242/dev.099382>, PMID: 24257623
- Komori H**, Xiao Q, Janssens DH, Dou Y, Lee CY. 2014b. Trithorax maintains the functional heterogeneity of neural stem cells through the transcription factor buttonhead. *eLife* **4**:e03502. DOI: <https://doi.org/10.7554/eLife.03502>
- Komori H**, Golden KL, Kobayashi T, Kageyama R, Lee CY. 2018. Multilayered gene control drives timely exit from the stem cell state in uncommitted progenitors during *Drosophila* asymmetric neural stem cell division. *Genes & Development* **32**:1550–1561. DOI: <https://doi.org/10.1101/gad.320333.118>, PMID: 30463902
- Kovač K**, Sauer A, Mačinković I, Awe S, Finkernagel F, Hoffmeister H, Fuchs A, Müller R, Rathke C, Längst G, Brehm A. 2018. Tumour-associated missense mutations in the dMi-2 ATPase alters nucleosome remodelling properties in a mutation-specific manner. *Nature Communications* **9**:2112. DOI: <https://doi.org/10.1038/s41467-018-04503-2>, PMID: 29844320
- Lee CY**, Robinson KJ, Doe CQ. 2006a. Lgl, pins and aPKC regulate neuroblast self-renewal versus differentiation. *Nature* **439**:594–598. DOI: <https://doi.org/10.1038/nature04299>, PMID: 16357871
- Lee CY**, Wilkinson BD, Siegrist SE, Wharton RP, Doe CQ. 2006b. Brat is a miranda cargo protein that promotes neuronal differentiation and inhibits neuroblast self-renewal. *Developmental Cell* **10**:441–449. DOI: <https://doi.org/10.1016/j.devcel.2006.01.017>, PMID: 16549393
- Levkowitz G**, Zeller J, Sirotkin HI, French D, Schilbach S, Hashimoto H, Hibi M, Talbot WS, Rosenthal A. 2003. Zinc finger protein *too few* controls the development of monoaminergic neurons. *Nature Neuroscience* **6**:28–33. DOI: <https://doi.org/10.1038/nn979>, PMID: 12469125
- Moore AW**, Jan LY, Jan YN. 2002. Hamlet, a binary genetic switch between single- and multiple- dendrite neuron morphology. *Science* **297**:1355–1358. DOI: <https://doi.org/10.1126/science.1072387>, PMID: 12193790
- Namba T**, Dóczy J, Pinson A, Xing L, Kalebic N, Wilsch-Bräuninger M, Long KR, Vaid S, Lauer J, Bogdanova A, Borgonovo B, Shevchenko A, Keller P, Drechsel D, Kurzchalia T, Wimberger P, Chinopoulos C, Huttner WB.

2020. Human-Specific ARHGAP11B acts in mitochondria to expand neocortical progenitors by glutaminolysis. *Neuron* **105**:867–881. DOI: <https://doi.org/10.1016/j.neuron.2019.11.027>, PMID: 31883789
- Neumüller RA, Richter C, Fischer A, Novatchkova M, Neumüller KG, Knoblich JA. 2011. Genome-wide analysis of self-renewal in *Drosophila* neural stem cells by transgenic RNAi. *Cell Stem Cell* **8**:580–593. DOI: <https://doi.org/10.1016/j.stem.2011.02.022>, PMID: 21549331
- Pfeiffer BD, Jenett A, Hammonds AS, Ngo TT, Misra S, Murphy C, Scully A, Carlson JW, Wan KH, Lavery TR, Mungall C, Svirskas R, Kadonaga JT, Doe CQ, Eisen MB, Celniker SE, Rubin GM. 2008. Tools for neuroanatomy and neurogenetics in *Drosophila*. *PNAS* **105**:9715–9720. DOI: <https://doi.org/10.1073/pnas.0803697105>, PMID: 18621688
- Ronan JL, Wu W, Crabtree GR. 2013. From neural development to cognition: unexpected roles for chromatin. *Nature Reviews Genetics* **14**:347–359. DOI: <https://doi.org/10.1038/nrg3413>, PMID: 23568486
- Shimada IS, Acar M, Burgess RJ, Zhao Z, Morrison SJ. 2017. Prdm16 is required for the maintenance of neural stem cells in the postnatal forebrain and their differentiation into ependymal cells. *Genes & Development* **31**:1134–1146. DOI: <https://doi.org/10.1101/gad.291773.116>, PMID: 28698301
- Sun G, Cui Q, Shi Y. 2017. Nuclear receptor TLX in development and diseases. *Current Topics in Developmental Biology* **125**:257–273. DOI: <https://doi.org/10.1016/bs.ctdb.2016.12.003>, PMID: 28527574
- Tsuboi M, Hirabayashi Y, Gotoh Y. 2019. Diverse gene regulatory mechanisms mediated by polycomb group proteins during neural development. *Current Opinion in Neurobiology* **59**:164–173. DOI: <https://doi.org/10.1016/j.conb.2019.07.003>
- Weng M, Golden KL, Lee CY. 2010. dFezf/Earmuff maintains the restricted developmental potential of intermediate neural progenitors in *Drosophila*. *Developmental Cell* **18**:126–135. DOI: <https://doi.org/10.1016/j.devcel.2009.12.007>, PMID: 20152183
- Xiao Q, Komori H, Lee CY. 2012. Klumpfuss distinguishes stem cells from progenitor cells during asymmetric neuroblast division. *Development* **139**:2670–2680. DOI: <https://doi.org/10.1242/dev.081687>, PMID: 22745313
- Xie Y, Li X, Zhang X, Mei S, Li H, Urso A, Zhu S. 2014. The *Drosophila* Sp8 transcription factor buttonhead prevents premature differentiation of intermediate neural progenitors. *eLife* **3**:e03596. DOI: <https://doi.org/10.7554/eLife.03596>
- Yang CP, Fu CC, Sugino K, Liu Z, Ren Q, Liu LY, Yao X, Lee LP, Lee T. 2016. Transcriptomes of lineage-specific *Drosophila* neuroblasts profiled by genetic targeting and robotic sorting. *Development* **143**:411–421. DOI: <https://doi.org/10.1242/dev.129163>, PMID: 26700685
- Zacharioudaki E, Housden BE, Garinis G, Stojnic R, Delidakis C, Bray SJ. 2016. Genes implicated in stem cell identity and temporal programme are directly targeted by notch in neuroblast tumours. *Development* **143**:219–231. DOI: <https://doi.org/10.1242/dev.126326>, PMID: 26657768
- Zhu S, Barshow S, Wildonger J, Jan LY, Jan YN. 2011. Ets transcription factor pointed promotes the generation of intermediate neural progenitors in *Drosophila* larval brains. *PNAS* **108**:20615–20620. DOI: <https://doi.org/10.1073/pnas.1118595109>, PMID: 22143802

## Appendix 1

Appendix 1—key resources table

Reagent type (species) or resource	Designation	Source or reference	Identifiers	Additional information
Antibody	anti-GFP (Chicken polyclonal)	Aves Labs, INC.	Cat#GFP-1020, RRID:AB_2307313	IF(1:2000)
Antibody	anti-V5 (Mouse monoclonal)	ThermoFisher Scientific	Cat#R960-25, RRID:AB_2556564	IF(1:500)
Antibody	anti-Ase (Rabbit polyclonal)	<b>Weng et al., 2010</b> doi: <a href="https://doi.org/10.1016/j.devcel.2009.12.007">10.1016/j.devcel.2009.12.007</a> .		IF(1:400)
Antibody	anti-Hamlet (Rabbit polyclonal)	<b>Eroglu et al., 2014</b> doi: <a href="https://doi.org/10.1016/j.cell.2014.01.053">10.1016/j.cell.2014.01.053</a> .		IF(1:50)
Antibody	anti-Dpn (Rat monoclonal)	<b>Lee et al., 2006a</b> doi: <a href="https://doi.org/10.1038/nature04299">10.1038/nature04299</a> .	clone 11D1BC7.14	IF(1:2)
Antibody	Alexa Fluor 488 AffiniPure Anti-Chicken IgY (IgG) (H+L) (Donkey polyclonal)	Jackson Immuno Research Laboratories, INC.	Cat#703-545-155, RRID:AB_2340375	IF(1:500)
Antibody	Alexa Fluor 647 AffiniPure anti-Rat IgG (H+L) (Goat polyclonal)	Jackson Immuno Research Laboratories, INC.	Cat#112-605-167 RRID:AB_2338404	IF(1:500)
Antibody	anti-Mouse IgG (H+L) Highly Cross-Adsorbed Secondary Antibody, Alexa Fluor 488 (Goat polyclonal)	ThermoFisher Scientific	Cat#A-11029, RRID:AB_2534088	IF(1:500)
Antibody	anti-Rabbit IgG (H+L) Highly Cross-Adsorbed Secondary Antibody, Alexa Fluor 488 (Goat polyclonal)	ThermoFisher Scientific	Cat#A-11034, RRID:AB_2576217	IF(1:500)
Antibody	anti-Rabbit IgG (H+L) Highly Cross-Adsorbed Secondary Antibody, Alexa Fluor 546 (Goat polyclonal)	ThermoFisher Scientific	Cat#A-11035, RRID:AB_2534093	IF(1:500)
Other	Rhodamine Phalloidin	ThermoFisher Scientific	Cat#R415	IF(1:100)
Genetic reagent (D. melanogaster)	<i>brat</i> <sup>11</sup> /CyO, Actin-GFP	<b>Lee et al., 2006b</b> doi: <a href="https://doi.org/10.1016/j.devcel.2006.01.017">10.1016/j.devcel.2006.01.017</a> .		
Genetic reagent (D. melanogaster)	<i>w</i> <sup>1118</sup> ; <i>Df</i> (2L) <i>Exel8040</i> /CyO	Bloomington Drosophila Stock Center	BDSC: 7847 FlyBase: FBst0007847; RRID:BDSC_7847	FlyBase symbol: <i>Df</i> (2L) <i>Exel8040</i> /CyO

Continued on next page

Appendix 1—key resources table continued

Reagent type (species) or resource	Designation	Source or reference	Identifiers	Additional information
Genetic reagent (D. melanogaster)	$y^1$ , M{vas-int.Dm}ZH-2A w <sup>*</sup> ; M{UAS-insb <sup>FL</sup> -myc}ZH-86Fb	<b>Komori et al., 2018</b> doi: <a href="https://doi.org/10.1101/gad.320333.118">10.1101/gad.320333.118</a> .		
Genetic reagent (D. melanogaster)	Wor-Gal4(II)	<b>Lee et al., 2006a</b> doi: <a href="https://doi.org/10.1038/nature04299">10.1038/nature04299</a> .		
Genetic reagent (D. melanogaster)	Wor-Gal4(III)	<b>Weng et al., 2010</b> doi: <a href="https://doi.org/10.1016/j.devcel.2009.12.007">10.1016/j.devcel.2009.12.007</a> .		
Genetic reagent (D. melanogaster)	$y^1$ , w <sup>*</sup> ; P{tubPGAL80}LL10, P{neoFRT}40A/CyO	Bloomington Drosophila Stock Center	BDSC: 5192 FlyBase: FBst0005192; RRID:BDSC_5192	FlyBase symbol: $y^1$ , w <sup>*</sup> ; P{tubPGAL80}LL10, P{neoFRT}40A/CyO
Genetic reagent (D. melanogaster)	P{hsFLP} <sup>1</sup> , P{tubP-GAL80}LL1, w <sup>*</sup> , P{neoFRT}19A; P{UAS-mCD8::GFP.L}LL5	Bloomington Drosophila Stock Center	BDSC: 5134 FlyBase: FBst0005134; RRID:BDSC_5134_	FlyBase symbol: P{hsFLP} <sup>1</sup> , P{tubP-GAL80}LL1, w <sup>*</sup> , P{neoFRT}19A; P{UAS-mCD8::GFP.L}LL5
Genetic reagent (D. melanogaster)	$y^1$ w <sup>*</sup> ; PBac{y[+mDint2]w[+mC]=tll EGFP.S}VK00037	Bloomington Drosophila Stock Center	BDSC: 30874 FlyBase: FBst0030874; RRID:BDSC_30874	FlyBase symbol: $y^1$ w <sup>*</sup> ; PBac{y[+mDint2]w[+mC]=tll EGFP.S}VK00037
Genetic reagent (D. melanogaster)	Erm-Gal4 (II)	<b>Pfeiffer et al., 2008</b> doi: <a href="https://doi.org/10.1073/pnas.0803697105">10.1073/pnas.0803697105</a> .		
Genetic reagent (D. melanogaster)	Erm-Gal4 (III)	<b>Pfeiffer et al., 2008</b> doi: <a href="https://doi.org/10.1073/pnas.0803697105">10.1073/pnas.0803697105</a> .		
Genetic reagent (D. melanogaster)	tll <sup>RNAi</sup> ; $y^1$ sc <sup>*</sup> v <sup>1</sup> sev <sup>21</sup> ; P{TRiP.HMS01316}attP2	Bloomington Drosophila Stock Center	BDSC: 34329 FlyBase: FBst0034329; RRID:BDSC_34329	FlyBase symbol: $y^1$ sc <sup>*</sup> v <sup>1</sup> sev <sup>21</sup> ; P{TRiP.HMS01316}attP2
Genetic reagent (D. melanogaster)	M{UAS-tll.ORF-VN}ZH-86Fb	FlyORF	F004752 FBst0502964; RRID:FlyORF_F004752	FlyBase symbol: M{UAS-tll.ORF-VN}ZH-86Fb
Genetic reagent (D. melanogaster)	Ase-Gal80 (II)	<b>Neumüller et al., 2011</b> doi: <a href="https://doi.org/10.1016/j.stem.2011.02.022">10.1016/j.stem.2011.02.022</a> .		
Genetic reagent (D. melanogaster)	erm <sup>1</sup> /CyO, Act-GFP	<b>Weng et al., 2010</b> doi: <a href="https://doi.org/10.1016/j.devcel.2009.12.007">10.1016/j.devcel.2009.12.007</a> .		
Genetic reagent (D. melanogaster)	erm <sup>2</sup> /CyO, Act-GFP	<b>Weng et al., 2010</b> doi: <a href="https://doi.org/10.1016/j.devcel.2009.12.007">10.1016/j.devcel.2009.12.007</a> .		
Genetic reagent (D. melanogaster)	UAS-erm	<b>Weng et al., 2010</b> doi: <a href="https://doi.org/10.1016/j.devcel.2009.12.007">10.1016/j.devcel.2009.12.007</a> .		

Continued on next page

Appendix 1—key resources table continued

Reagent type (species) or resource	Designation	Source or reference	Identifiers	Additional information
Genetic reagent (D. melanogaster)	PBac{erm-flag4C(g)}VK33	<b>Janssens and Lee, 2014</b> doi: <a href="https://doi.org/10.1242/dev.106534">10.1242/dev.106534</a> .		
Genetic reagent (D. melanogaster)	D <sup>RNAi</sup> ; y <sup>1</sup> v <sup>1</sup> ; P{TRiP.JF02115}attP2	Bloomington Drosophila Stock Center	BDSC: 26217 FlyBase: FBst0026217; RRID: <a href="https://rrid.nlm.nih.gov/rrid/BDSC_26217">BDSC_26217</a>	FlyBase symbol: y <sup>1</sup> v <sup>1</sup> ; P{TRiP.JF02115}attP2
Genetic reagent (D. melanogaster)	Ase <sup>RNAi</sup> ; y <sup>1</sup> sc* v <sup>1</sup> sev <sup>21</sup> ; P{TRiP.HMS02847}attP2	Bloomington Drosophila Stock Center	BDSC: 44552 FlyBase: FBst0044552; RRID: <a href="https://rrid.nlm.nih.gov/rrid/BDSC_44552">BDSC_44552</a>	FlyBase symbol: y <sup>1</sup> sc* v <sup>1</sup> sev <sup>21</sup> ; P{TRiP.HMS02847}attP2
Genetic reagent (D. melanogaster)	ham <sup>RNAi</sup> ; y <sup>1</sup> v <sup>1</sup> ; P{TRiP.JF02270}attP2	Bloomington Drosophila Stock Center	BDSC: 26728 FlyBase: FBst0026728; RRID: <a href="https://rrid.nlm.nih.gov/rrid/BDSC_26728">BDSC_26728</a>	FlyBase symbol: y <sup>1</sup> v <sup>1</sup> ; P{TRiP.JF02270}attP2
Genetic reagent (D. melanogaster)	ham <sup>RNAi</sup> ; y <sup>1</sup> sc* v <sup>1</sup> sev <sup>21</sup> ; P{y[+t7.7] v[+t1.8]=TRiP.HMS00470}attP2	Bloomington Drosophila Stock Center	BDSC: 32470 FlyBase: FBst0032470; RRID: <a href="https://rrid.nlm.nih.gov/rrid/BDSC_32470">BDSC_32470</a>	FlyBase symbol: y <sup>1</sup> sc* v <sup>1</sup> sev <sup>21</sup> ; P{y[+t7.7] v[+t1.8]=TRiP.HMS00470}attP2
Genetic reagent (D. melanogaster)	Opa <sup>RNAi</sup> ; y <sup>1</sup> sc* v <sup>1</sup> sev <sup>21</sup> ; P{TRiP.HMS01185}attP2/TM3, Sb <sup>1</sup>	Bloomington Drosophila Stock Center	BDSC: 34706 FlyBase: FBst0034706; RRID: <a href="https://rrid.nlm.nih.gov/rrid/BDSC_34706">BDSC_34706</a>	FlyBase symbol: y <sup>1</sup> sc* v <sup>1</sup> sev <sup>21</sup> ; P{TRiP.HMS01185}attP2/ TM3, Sb <sup>1</sup>
Genetic reagent (D. melanogaster)	w <sup>1118</sup> ; Df(2L)Exel7071/CyO	Bloomington Drosophila Stock Center	BDSC: 7843 FlyBase: FBst0007843; RRID: <a href="https://rrid.nlm.nih.gov/rrid/BDSC_7843">BDSC_7843</a>	FlyBase symbol: w <sup>1118</sup> ; Df(2L)Exel7071/CyO
Genetic reagent (D. melanogaster)	ham <sup>SKI</sup> , FRT40A/CyO	This paper		A new hamlet mutant fly line
Genetic reagent (D. melanogaster)	P{w[+mW.hs]=GawB}elav[C155], P{w[+mC]=UAS-mCD8::GFP.L}Ptp4E[LL4], P{ry[+t7.2]=hsFLP}1, w[*]	Bloomington Drosophila Stock Center	BDSC: 5146 FlyBase: FBst0005146; RRID: <a href="https://rrid.nlm.nih.gov/rrid/BDSC_5146">BDSC_5146</a>	FlyBase symbol: P{w[+mW.hs]=GawB}elav [C155], P{w[+mC]=UAS-mCD8::GFP.L}Ptp4E[LL4], P{ry[+t7.2]=hsFLP}1, w[*]
Genetic reagent (D. melanogaster)	w <sup>1118</sup> ; P{w[+mC]=UAS-Dcr-2.D}2	Bloomington Drosophila Stock Center	BDSC: 24650 FlyBase: FBst00024650; RRID: <a href="https://rrid.nlm.nih.gov/rrid/BDSC_24650">BDSC_24650</a>	FlyBase symbol: w <sup>1118</sup> ; P{w[+mC]=UAS-Dcr-2.D}2
Genetic reagent (D. melanogaster)	w*; P{w[+mC]=tubP-GAL8 <sup>ts</sup> }2/TM2	Bloomington Drosophila Stock Center	BDSC: 7017 FlyBase: FBst00024650; RRID: <a href="https://rrid.nlm.nih.gov/rrid/BDSC_7017">BDSC_7017</a>	FlyBase symbol: w*; P{w[+mC]=tubP- GAL8 <sup>ts</sup> }2/ TM2
Genetic reagent (D. melanogaster)	ham <sup>1</sup> , FRT40A/CyO	<b>Moore et al., 2002</b> doi: <a href="https://doi.org/10.1126/science.1072387">10.1126/science.1072387</a> .		
Genetic reagent (D. melanogaster)	UAS-ham	<b>Moore et al., 2002</b> doi: <a href="https://doi.org/10.1126/science.1072387">10.1126/science.1072387</a> .		

Continued on next page

Appendix 1—key resources table continued

Reagent type (species) or resource	Designation	Source or reference	Identifiers	Additional information
Genetic reagent (D. melanogaster)	RNAi of Notch: $y^1, v^1$ ; $P\{y+t7.7v+t1.8=TRiP.HMS00001\}attP2$	Bloomington Drosophila Stock Center	BDSC: 33611 FlyBase: FBst0033611; RRID:BDSC_33611	FlyBase symbol: $y^1, v^1$ ; $P\{y+t7.7v+t1.8=TRiP.HMS00001\}attP2$
Genetic reagent (D. melanogaster)	Oregon-R-C	Bloomington Drosophila Stock Center	BDSC: 5 FlyBase: FBst0000005; RRID:BDSC_5	FlyBase symbol: Oregon-R-C
Genetic reagent (D. melanogaster)	$P\{hsFLP\}^1, y^1 w^*$ ; $P\{UAS-N.intra.GS\}2/CyO$ ; MKRS/TM2	Bloomington Drosophila Stock Center	BDSC: 52008 FlyBase: FBst0052008; RRID:BDSC_52008	FlyBase symbol: $P\{hsFLP\}^1, y^1 w^*$ ; $P\{UAS-N.intra.GS\}2/CyO$ ; MKRS/TM2
Genetic reagent (D. melanogaster)	$y^1$ ; $M\{vas-int.Dm\}ZH-2A w^*$ ; $M\{UAS-ham^{AC-ZF-myc}\}ZH-86Fb$	This paper		Transgene expressing Hamlet mutant form of the C-terminal zinc finger deletion version
Genetic reagent (D. melanogaster)	$y^1$ ; $M\{vas-int.Dm\}ZH-2A w$ ; $M\{UAS-ERD::ham^{N-ZF-myc}\}ZH-86Fb$	This paper		Transgene expressing Hamlet the N-terminal zinc finger fused with ERD transcriptional repression domain
Genetic reagent (D. melanogaster)	$y^1$ ; $M\{vas-int.Dm\}ZH-2A w$ ; $M\{UAS-VP-16::ham^{N-ZF-myc}\}ZH-86Fb$	This paper		Transgene expressing Hamlet the N-terminal zinc finger fused with VP16 transcriptional activation domain
Genetic reagent (D. melanogaster)	$cu^1, tll^{49}/TM3, P\{ftz/lacC\}SC^1, Sb^1, Ser^1$	Bloomington Drosophila Stock Center	BDSC: 7093 FlyBase: FBst007093; RRID:BDSC_7093	FlyBase symbol: $cu^1, tll^{49}/TM3, P\{ftz/lacC\}SC^1, Sb^1, Ser^1$
Genetic reagent (D. melanogaster)	$st^1 e^1 tll^1/TM3, Sb^1$	Bloomington Drosophila Stock Center	BDSC: 2729 FlyBase: FBst002729; RRID:BDSC_2729	FlyBase symbol: $st^1 e^1 tll^1/TM3, Sb^1$
Genetic reagent (D. melanogaster)	$ham^{SK4}, FRT40A/CyO$	Bloomington Drosophila Stock Center	BDSC: 34329 FlyBase: FBst0034329; RRID:BDSC_34329	FlyBase symbol: $y^1 sc^* v^1 sev^{21}$ ; $P\{TRiP.HMS01316\}attP2$
Genetic reagent (D. melanogaster)	$hdac3^{RNAi}: y^1 sc^* v^1 sev^{21}$ ; $P\{TRiP.HMS00087\}attP2$	Bloomington Drosophila Stock Center	BDSC: 34778 FlyBase: FBst0034778; RRID:BDSC_34778	FlyBase symbol: $hdac3^{RNAi}: y^1 sc^* v^1 sev^{21}$ ; $P\{TRiP.HMS00087\}attP2$
Genetic reagent (D. melanogaster)	$Su(z)12^{RNAi}: y^1 sc^* v^1 sev^{21}$ ; $P\{TRiP.HMS00280\}attP2/TM3, Sb^1$	Bloomington Drosophila Stock Center	BDSC: 33402 FlyBase: FBst0033402; RRID:BDSC_33402	FlyBase symbol: $y^1 sc^* v^1 sev^{21}$ ; $P\{TRiP.HMS00280\}attP2/TM3, Sb^1$
Genetic reagent (D. melanogaster)	$Su(var)3-3^{RNAi}: y^1 sc^* v^1 sev^{21}$ ; $P\{TRiP.HMS00638\}attP2$	Bloomington Drosophila Stock Center	BDSC: 32853 FlyBase: FBst0032853; RRID:BDSC_32853	FlyBase symbol: $y^1 sc^* v^1 sev^{21}$ ; $P\{TRiP.HMS00638\}attP2$
Genetic reagent (D. melanogaster)	$Su(var)205^{RNAi}: y^1 sc^* v^1 sev^{21}$ ; $P\{TRiP.GL00531\}attP40$	Bloomington Drosophila Stock Center	BDSC: 36792 FlyBase: FBst0146447; RRID:BDSC_36792	FlyBase symbol: $y^1 sc^* v^1 sev^{21}$ ; $P\{TRiP.GL00531\}attP40$

Continued on next page

## Appendix 1—key resources table continued

Reagent type (species) or resource	Designation	Source or reference	Identifiers	Additional information
Genetic reagent (D. melanogaster)	UAS-Mi-2 <sup>DN</sup>	<b>Kovač et al., 2018</b> doi: <a href="https://doi.org/10.1038/s41467-018-04503-2">10.1038/s41467-018-04503-2</a> .		
Genetic reagent (D. melanogaster)	UAS-Mi-brm <sup>DN</sup>	<b>Herr et al., 2010</b> doi: <a href="https://doi.org/10.1016/j.ydbio.2010.04.006">10.1016/j.ydbio.2010.04.006</a> .		
Genetic reagent (D. melanogaster)	<i>In(1)wm4; Su(var)3-91/TM3, Sb<sup>1</sup> Ser<sup>1</sup></i>	Bloomington <i>Drosophila</i> Stock Center	BDSC: 6209 FlyBase: FBst0006209; RRID:BDSC_6209	FlyBase symbol: <i>In(1)wm4; Su(var)3-91/TM3, Sb<sup>1</sup> Ser<sup>1</sup></i>
Genetic reagent (D. melanogaster)	<i>w<sup>1118</sup>; PBac{Sp1-EGFP.S}VK00033</i>	Bloomington <i>Drosophila</i> Stock Center	BDSC: 38669 FlyBase: FBst0038669; RRID:BDSC_38669	FlyBase symbol: <i>w<sup>1118</sup>; PBac{Sp1-EGFP.S}VK00033</i>
Sequenced-based reagent	Ham_F	<b>Eroglu et al., 2014</b> doi: <a href="https://doi.org/10.1016/j.cell.2014.01.053">10.1016/j.cell.2014.01.053</a> .	PCR primers	atagatcctttggccagcagac
Sequenced-based reagent	Ham_R	<b>Eroglu et al., 2014</b> doi: <a href="https://doi.org/10.1016/j.cell.2014.01.053">10.1016/j.cell.2014.01.053</a> .	PCR primers	agtactcctcctttcggaat
Sequenced-based reagent	Ase_F	<b>Komori et al., 2014b</b> doi: <a href="https://doi.org/10.7554/eLife.03502">10.7554/eLife.03502</a> .	PCR primers	agcccgtagcttctacgac
Sequenced-based reagent	Ase_R	<b>Komori et al., 2014b</b> doi: <a href="https://doi.org/10.7554/eLife.03502">10.7554/eLife.03502</a> .	PCR primers	gcatcgatcatgctctcgtc
Sequenced-based reagent	D_F	This paper	PCR primers	gcggcgcggtcaacaat
Sequenced-based reagent	D_R	This paper	PCR primers	tgccgctacagcgaagggt
Sequenced-based reagent	Erm_F	<b>Eroglu et al., 2014</b> doi: <a href="https://doi.org/10.1016/j.cell.2014.01.053">10.1016/j.cell.2014.01.053</a> .	PCR primers	gttacggccaggcatcgggtcaa
Sequenced-based reagent	Erm_R	<b>Eroglu et al., 2014</b> doi: <a href="https://doi.org/10.1016/j.cell.2014.01.053">10.1016/j.cell.2014.01.053</a> .	PCR primers	gggccaggcgggattactcgtctc
Sequenced-based reagent	PntP1_F	<b>Komori et al., 2014b</b> doi: <a href="https://doi.org/10.7554/eLife.03502">10.7554/eLife.03502</a> .	PCR primers	ggcagtagggcagcaccac
Sequenced-based reagent	PntP1_R	<b>Komori et al., 2014b</b> doi: <a href="https://doi.org/10.7554/eLife.03502">10.7554/eLife.03502</a> .	PCR primers	ctcaacgccccaccagatt

Continued on next page

## Appendix 1—key resources table continued

Reagent type (species) or resource	Designation	Source or reference	Identifiers	Additional information
Sequenced-based reagent	Dpn_F	<b>Komori et al., 2014b</b> doi: <a href="https://doi.org/10.7554/eLife.03502">10.7554/eLife.03502</a> <b>Komori et al., 2014b</b>	PCR primers	catcatgccgaacacaggtt
Sequenced-based reagent	Dpn_R	<b>Komori et al., 2014b</b>	PCR primers	gaagattggccggaactgag
Recombinant DNA reagent	<i>pUAST-ham<sup>ΔC-ZF-</sup>myc-attB (plasmid)</i>	This paper		Plasmid DNA of a transgene expressing Hamlet mutant form of the C-terminal zinc finger deletion version
Recombinant DNA reagent	<i>pUAST-ERD::ham<sup>N-ZF-</sup>myc-attB (plasmid)</i>	This paper		Plasmid DNA of a transgene expressing Hamlet the N-terminal zinc finger fused with ERD transcriptional repression domain
Recombinant DNA reagent	<i>pUAST-VP16::ham<sup>N-ZF-</sup>myc-attB (plasmid)</i>	This paper		Plasmid DNA of a transgene expressing Hamlet the N-terminal zinc finger fused with VP16 transcriptional activation domain
Software, algorithm	LAS AF	Leica Microsystems	RRID: <a href="https://rrid.nlm.nih.gov/rrid/SCR_013673">SCR_013673</a>	
Software, algorithm	ImageJ 1.50 g	National Institute of Health	RRID: <a href="https://rrid.nlm.nih.gov/rrid/SCR_003070">SCR_003070</a>	